Development 138, 2235-2247 (2011) doi:10.1242/dev.059105

p45NF-E2 represses Gcm1 in trophoblast cells to regulate syncytium formation, placental vascularization and embryonic growth

Muhammed Kashif[1], Andrea Hellwig[2], Alexandre Kolleker[3], Khurrum Shahzad[1], Hongjie Wang[1,4], Siegfried Lang[5], Juliane Wolter[1], Madhusudhan Thati[1], Ilya Vinnikov[1], Angelika Bierhaus[1], Peter P. Nawroth[1] and Berend Isermann[1,*,†]

SUMMARY

Absence of the leucine zipper transcription factor p45NF-E2 results in thrombocytopenia, impaired placental vascularization and intrauterine growth restriction (IUGR) in mice. The mechanism underlying the p45NF-E2-dependent placental defect and IUGR remains unknown. Here, we show that the placental defect and IUGR of *p45NF-E2* (*Nfe2*) null mouse embryos is unrelated to thrombocytopenia, establishing that embryonic platelets and platelet-released mediators are dispensable for placentation. Rather, p45NF-E2, which was hitherto thought to be specific to hematopoietic cells, is expressed in trophoblast cells, where it is required for normal syncytiotrophoblast formation, placental vascularization and embryonic growth. Expression of p45NF-E2 in labyrinthine trophoblast cells colocalizes with that of Gcm1, a transcription factor crucial for syncytiotrophoblast formation. In the absence of p45NF-E2, the width of syncytiotrophoblast layer 2 and the expression of Gcm1 and Gcm1-dependent genes (*Synb* and *Cebpa*) are increased. In vitro, p45NF-E2 deficiency results in spontaneous syncytiotrophoblast formation, which can be reversed by Gcm1 knockdown. Increased Gcm1 expression in the absence of p45NF-E2 is dependent on enhanced protein acetylation, including post-translational modification of Gcm1. Increasing and inhibiting acetylation in the placenta of wild-type control embryos phenocopies and corrects, respectively, the changes observed in p45NF-E2-deficient embryos. These studies identify a novel function of p45NF-E2 during placental development: in trophoblast cells, p45NF-E2 represses Gcm1 and syncytiotrophoblast formation via acetylation.

KEY WORDS: Syncytiotrophoblast differentiation, Placental morphogenesis, Platelets, NF-E2, Nfe2, Gcm1, Acetylation, Mouse

INTRODUCTION

Intrauterine growth restriction (IUGR) is a frequent but incompletely understood pregnancy complication that occurs in ~8% of pregnancies (McIntire et al., 1999). Knockout studies in mice have identified a number of genes required for normal placentation (Cross, 2005), including genes that regulate the activity of the coagulation system (Brenner and Kupferminc, 2003; Sood and Weiler, 2003). The developmental function of the coagulation system is at least partially independent of its well-known hemostatic function in the regulation of the fibrin-platelet interaction, as embryos simultaneously lacking fibrinogen and carrying a severe platelet defect develop normally (Camerer et al., 2004; Palumbo et al., 2004). The notable exception is an IUGR and impaired placental vascularization observed in *p45NF-E2* (*Nfe2* – Mouse Genome Informatics) null mice lacking platelets (Palumbo et al., 2004). A similar developmental defect is not detectable in embryos with normal platelet numbers but disturbed platelet function [*Par4* or *Gαq* (*F2rl3* or *Gnaq* – Mouse Genome Informatics) null mice] (Camerer et al., 2004; Palumbo et al., 2004). A developmental role for platelets is not necessarily precluded by the normal development of $Par4^{-/-}$ or $G\alpha q^{-/-}$ embryos, as platelets lacking Par4 or Gαq can still be activated (Ohlmann et al., 2000; Sambrano et al., 2001). This raises the question of whether embryonic platelets have an as yet undefined developmental function or whether p45NF-E2 has a developmental function that is independent of platelets.

NF-E2 belongs to the basic region leucine zipper (bZip) superfamily of transcription factors. It consists of two subunits: a 45 kDa (p45) subunit thought to be restricted to megakaryocytes, erythrocytes and mast cells; and a widely expressed 18 kDa (p18) subunit. Mice lacking p45NF-E2 display severe thrombocytopenia caused by a megakaryocyte maturation defect (Shivdasani et al., 1995). Megakaryocytes can be detected in the embryonic compartment as early as 7.5 days post-coitum (dpc) (Xu et al., 2001), and platelets may alter placental development through various mechanisms (Ohlsson et al., 1999; Sato et al., 2005). Hence, it is generally assumed, but remains to be shown, that the IUGR of p45NF-E2-deficient embryos results from the absence of embryonic platelets.

However, a role of the bZip transcription factor p45NF-E2 in placental development independent of platelets or megakaryocytes cannot currently be ruled out. Other bZip transcription factors, such as JunB, Fra1 (Fosl1), Tfeb (Tcfeb), Creb and Oasis (Creb3l1), regulate trophoblast differentiation or placental development (Schorpp-Kistner et al., 1999; Schreiber et al., 2000a; Schreiber et

[1]Department of Medicine I and Clinical Chemistry, University of Heidelberg, INF 410, 69120 Heidelberg, Germany. [2]Department of Neurobiology, Interdisciplinary Center for Neurosciences (IZN), University of Heidelberg, INF 364, 69120 Heidelberg, Germany. [3]Max-Planck-Institute for Medical Research, Jahnstraße 29, 69120 Heidelberg, Germany. [4]Department of Cardiology, Tongji Hospital, Tongji Medical College, Huazhong University of Science and Technology, Wuhan 430030, China. [5]Department of Internal Medicine I, Medical Faculty Mannheim, University of Heidelberg, 68167 Mannheim, Germany.

*Present address: Otto-von-Guericke-Universität Magdeburg, Medizinische Fakultät, Institut für Klinische Chemie und Pathobiochemie, Leipziger Str. 44, 39120 Magdeburg, Germany
†Author for correspondence (berend.isermann@med.ovgu.de)

Accepted 9 March 2011

al., 2000b; Schubert et al., 2008; Steingrimsson et al., 1998). Creb and Oasis regulate the expression of Gcm1, a key regulator of placental development that is required for chorioallantoic branching and syncytiotrophoblast formation (Anson-Cartwright et al., 2000). The stability and binding activity of Gcm1 are furthermore post-translationally regulated by acetylation. Hence, p45NF-E2 might regulate Gcm1 expression by interacting with other bZip transcription factors or by modulating acetylation.

In the current study we identify a novel function of p45NF-E2 in non-hematopoietic cells. In trophoblast cells, p45NF-E2 acts as a transcriptional repressor, reducing Gcm1-dependent syncytiotrophoblast differentiation by inhibiting acetylation.

MATERIALS AND METHODS

Materials

Cell culture media, fetal bovine serum, glutamine, penicillin/streptomycin mix, neuromycin, non-essential amino acids, sodium pyruvate, PCR4-TOPO cloning vector and pcDNA3.1/V5-His-TOPO vector were obtained from Invitrogen (Karlsruhe, Germany). ESGRO (LIF), thrombopoietin (Thpo), M2 medium and KSOM medium were purchased from R&D Systems (Wiesbaden-Nordstadt, Germany). P24 tag antigen ELISA and ChIP assay kits were from Biocat (Heidelberg, Germany). ECL reagent was from Amersham Biosciences (Little Chalfont, UK). Murine p45NF-E2 and Gcm1 shRNA constructs (pLKO1-NF-E2, pLKO1-Gcm1) and the murine Gcm1 full-length cDNA construct (pCMV-SPORT6-Gcm1) were from Open Biosystems (Huntsville, AL, USA). GoTaq DNA polymerase and the AP-1 consensus oligo sequence for electrophoretic mobility shift assay (EMSA) were from Promega (Mannheim, Germany). P45NF-E2 consensus oligo sequence for EMSA and rabbit polyclonal IgGs (NF-E2, CBP) and goat polyclonal IgG (Gcm1) were from Santa Cruz Biotechnology (Heidelberg, Germany). Rabbit polyclonal anti-acetylated lysine IgG antibody was from Cell Signaling (Boston, MA, USA). All primers were synthesized by Thermo Scientific (Langenselbold, Germany). All other materials were obtained from Sigma-Aldrich (Taufkirchen, Germany).

Mice and generation of tetraploid aggregation embryos

p45NF-E2$^{-/-}$ mice were kindly provided by R. Shivdasani (Harvard Medical School, Cambridge, MA, USA). CD-1 mice were from Charles River Laboratories (Sulzfeld, Germany). Aggregation of wild-type ES cells with tetraploid *p45NF-E2* embryos was achieved essentially as described previously (Isermann et al., 2001; Nagy et al., 1993). In brief, p45NF-E2-deficient mice were backcrossed for one generation onto the CD-1 background and then heterozygous *p45NF-E2* offspring (F1) were bred to generate *p45NF-E2*$^{-/-}$ embryos with a mixed C57Bl/6–CD-1 genetic background. These embryos were used to generate tetraploid embryos as previously described (Isermann et al., 2001). Tetraploid embryos were aggregated with clusters of 10-15 R1 wild-type ES cells (Isermann et al., 2001).

All animals were housed and the experiments were performed at the interdisciplinary biomedical research institution (IBF) at the University of Heidelberg, Germany, following standards and procedures approved by the local Animal Care and Use Committee (Regierungspräsidium Karlsruhe, Germany).

Timed matings and analyses of embryos and placental morphology

Placental and embryonic tissues were obtained from timed matings of *p45NF-E2*$^{+/-}$ females and *p45NF-E2*$^{-/-}$ males on a C57Bl/6 background. Embryonic tissue was used for genotyping. Half of the placental tissue was fixed in 4% buffered formalin while the other half was further divided and stored either in RNAlater (Ambion) or snap frozen in liquid nitrogen.

For analyses of gross placental morphology, placental sections were stained with *Bandeiraea simplicifolia* BS-I B4 (40 ng/μl) as previously described (Hemberger et al., 1999). Nuclear counterstaining was carried out with Hematoxylin and the spongiotrophoblast and labyrinthine layer area was measured by a blinded investigator using UTHSCSA ImageTool software on three placental sections per placenta. Hematoxylin and Eosin-stained placental sections were analyzed for vascular space quantification. In each section, at least ten randomly selected microscopic fields in the labyrinthine region from three nonconsecutive placental sections (magnification 20×) were acquired at 1280×960 pixel resolution using a digital camera (Nikon Digital Sight DS-U1) connected to a light microscope (Nikon Eclipse TE 2000). We implemented an image analysis routine using NIS Elements AR2.30 imaging software. Briefly, after acquisition, the images underwent an automated light analysis procedure and were given a color threshold to cover the area corresponding to the blood spaces lumen. The coverage percentage was calculated as the ratio between the number of pixels covered by the area defined by the threshold and the overall number of pixels in the image. Analyses were performed by a blinded investigator. Analysis of placental perfusion was performed essentially as previously described (Sood et al., 2007). Briefly, for analyses of embryonic perfusion, pregnant females were injected with 100 μl 25 mg/ml FITC-labeled dextran (molecular weight 2×10^6 Da) via the tail vein at 14.5 dpc. For analysis of embryonic perfusion, embryos with an intact yolk sac vasculature and placenta were isolated at 17.5 dpc and ~20 μl of FITC-labeled dextran was injected intracardially. The placenta was isolated after 15 minutes, embedded in tissue-freezing medium (Tissue-Tek) and flash frozen in a dry ice-ethanol bath. Micrographs of serial tissue sections were obtained using the same microscope, camera and software as above. The perfused area was quantified following a routine automated light analysis procedure with a color threshold to cover the FITC-positive, perfused area, similar to the procedure described above for the vascular space analyses.

Regular RT-PCR was performed using the following primers (5′ to 3′): actin, CTAGACTTCGAGCAGGAGATGG and GCTAGGAGCCAG-AGCAGTAATC; MafF, GTGCCTGAGTTCCTTCTGCT and CA-CAGTTGGGAGGTCTGCTT; MafG, GAGGAGCTGGAGAAGCAGAA and GAGCATCCGTCTTGGACTTT; and MafK, GCACACTC-AAGAACAGAGGC and CTGAGAAGGGTACAGAGGTGG.

Quantitative RT-PCR (qRT-PCR) was performed as previously described (Rudofsky et al., 2007). Initially, RT-PCR was performed (57°C for 1 minute, 72°C for 1 minute, 30 cycles) using the following primers (5′ to 3′): actin, CTAGACTTCGAGCAGGAGATGG and GCTAG-GAGCCAGAGCAGTAATC; Cebpa, CGCTGGTGATCAAACAAGAG and GTCACTGGTCAACTCCAGCA; Esx1, GTACCCGGACCT-GTTTGCTA and CTTGCTGCATTGGGTATGTG; Gcm1 coding sequence, GACTGCTCCACAGAGGAAGG and GGAGAGCCATAG-GTGAGCAG; p45NF-E2, CACCAAATACTCCCAGGTGATATG and AACTTGCCGGTAGATGACTTTAAT; PL-II, CTCCTTCT-CTGGGCAACTC and GGACTTGCTCGCTGTTTTC; Synb, TGAC-CTTGAAGTGGGTAGGG and TGACCTTGAAGTGGGTAGGG; and 4311, CAGGTACTTGAGACATGACTC and AGAGATTTCTT-AGACAATG. PCR fragments were cloned using the TOPO TA Cloning Kit (Invitrogen) and confirmed by sequencing. Generation of standard curves and evaluation of final data were performed as described (Rudofsky et al., 2007). All RT-PCRs were performed in triplicate.

AP-1 or p45NF-E2 binding activity was determined by EMSA as described previously (Bierhaus et al., 2001). Immunoblotting was performed as described (Isermann et al., 2007).

Chromatin immunoprecipitation (ChIP) and co-immunoprecipitation

ChIP was performed on placental tissue extracts using the EpiQuik ChIP Assay Kit for tissue following the manufacturer's instructions (Epigentek, Brooklyn, NY, USA). Gcm1 (third intron) primers were 5′-ATTC-GTGAATAAGTAGGGAGGA-3′ and 5′-GCTGATTCTGAGTCTGA-GGTGTC-3′. Co-immunoprecipitation was performed as described (Qiu et al., 2004).

Transmission electron microscopy

Placental tissues obtained at 16.5 dpc were fixed with 2.5% glutaraldehyde, 2.5% polyvidone 25, 0.1 M sodium cacodylate pH 7.4. After washing with 0.1 M sodium cacodylate buffer (pH 7.4), samples were post-fixed in the same buffer containing 2% osmium tetroxide and 1.5% potassium ferrocyanide for 1 hour, washed in water, contrasted en

bloc with uranyl acetate, dehydrated using an ascending series of ethanol and embedded in glycidyl ether 100-based resin. Ultrathin sections were cut with a Reichert Ultracut S ultramicrotome (Leica Microsystems, Wetzlar, Germany), contrasted with uranyl acetate and lead citrate, and were viewed with an EM 10 CR electron microscope (Carl Zeiss NTS, Oberkochen, Germany).

Mouse trophoblast cell culture and in vitro syncytium formation

Mouse trophoblast stem (TS) cells were obtained from J. Rossant (Hospital for Sick Children, Toronto, ON, Canada) and were maintained as stem cells or induced to differentiate as previously described (Isermann et al., 2003; Tanaka et al., 1998). Syncytiotrophoblast formation was monitored in nearly confluent TS cells differentiated for 6 days. In some cases, TS cells were differentiated in the presence of HDAC inhibitor [100 nM trichostatin A (TSA) or 2.5 mM sodium butyrate] (Maltepe et al., 2005) or HAT inhibitor (30 nM curcumin or 5 μM EGCG) (Balasubramanyam et al., 2004; Tachibana et al., 2004).

For quantification of syncytiotrophoblast formation, cells were incubated with 2.5 μm CellMask Deep Red (Invitrogen) for 5 minutes at 37°C and then fixed for 3 minutes in 3.75% formaldehyde at room temperature. Cells were counterstained with DAPI (0.5 μg/ml in PBS) for 10 minutes at room temperature in the dark. For quantification of syncytiotrophoblasts, at least 30 random images per slide were captured (UTHSCSA ImageTool software) and the frequency of syncytial cells observed in these random images was determined by a blinded investigator.

Generation of *Gcm1* mutants, knock-in and knockdown constructs

Murine p45NF-E2 (pLKO1-NF-E2) and Gcm1 (pLKO1-Gcm1) knockdown constructs containing shRNA for *p45NF-E2* or *Gcm1* cloned into the lentiviral plasmid vector pLKO1 were obtained from Open Biosystems. Gcm1 expression plasmid pLV-Gcm1 was generated by replacing the *EGFP* fragment (*Eco*RI/*Xho*I) of the plasmid pLV-EGFP [kindly provided by Masahito Ikawa, Osaka, Japan (Okada et al., 2007)] with full-length *Gcm1* cDNA (*Eco*RI/*Xho*I fragment; Open Biosystems). The p45NF-E2-expressing plasmid pLV-NF-E2 was generated by replacing *EGFP* in the plasmid pLV-EGFP with PCR-derived murine *p45NF-E2* cDNA. In detail, a p45NF-E2-coding PCR fragment was generated from wild-type 14.5 dpc placental cDNA using the forward primer 5′-TCAGCTGGCACAGTAGGATG-3′ and the reverse primer 5′-CATCAGAAGGGAATGAGGGA-3′ (57°C annealing temperature, 35 cycles). The fragment was cloned into pcDNA3.1/V5-His-TOPO, yielding the plasmid pTOPO-NF-E2. Subsequently, the EGFP coding sequence of pLV-EGFP was replaced by the *Bam*HI-*Xho*I fragment of pTOPO-NF-E2, yielding pLV-NF-E2, as confirmed by sequencing.

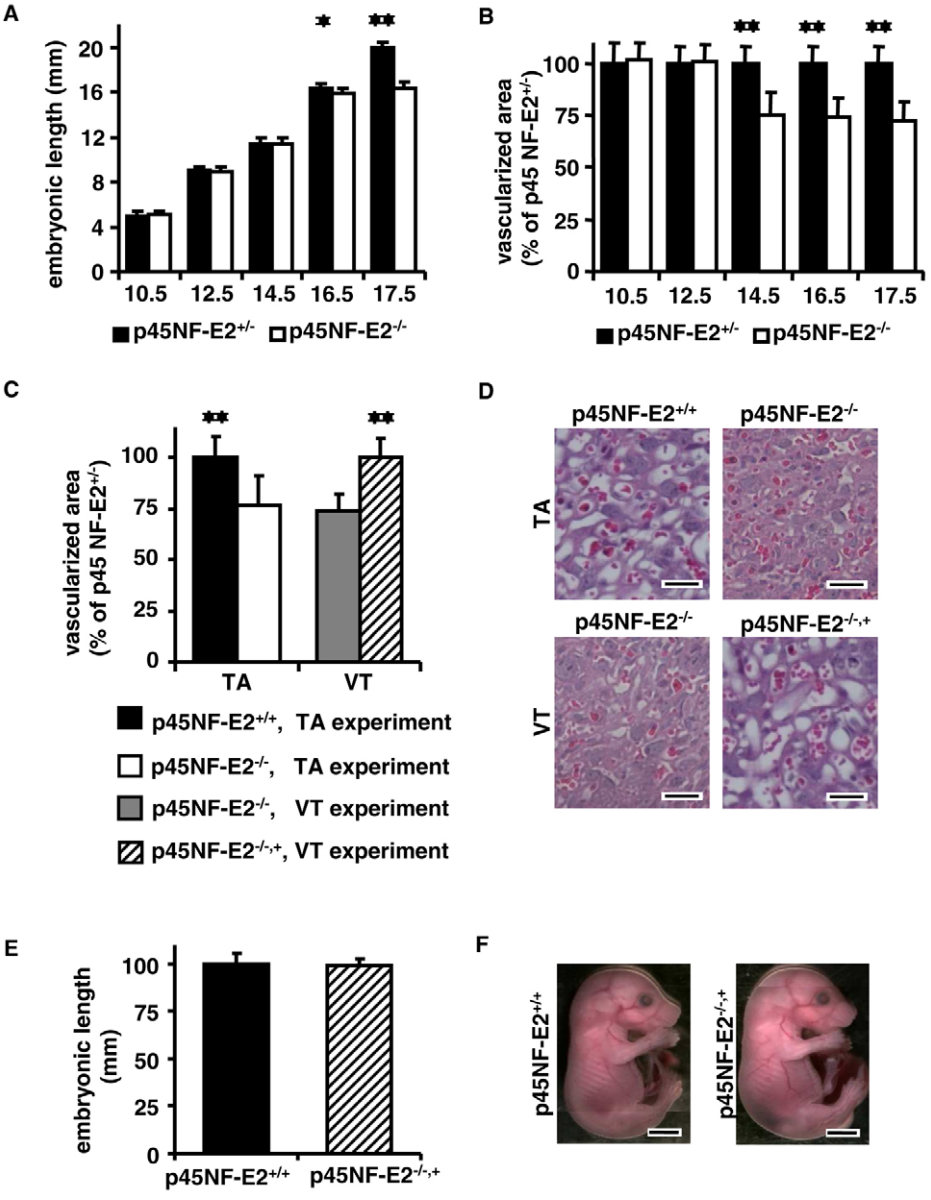

Fig. 1. p45NF-E2 deficiency in trophectodermal cells impairs placental vascularization. (**A**,**B**) Impairment of placental vascularization precedes embryonic growth retardation of *p45NF-E2*$^{-/-}$ mouse embryos. Bar charts summarizing embryonic length (A, $n \geq 27$ per group) and placental vascularized area (B, $n \geq 12$ per group) at various developmental stages. (**C**,**D**) Bar chart showing placental vascularized area (C) and representative images (D) of Hematoxylin and Eosin (HE)-stained placental sections (14.5 dpc). The placental genotype is shown. Restricted p45NF-E2 expression within the embryo proper (aggregation of tetraploid *p45NF-E2*$^{-/-}$ placenta with *p45NF-E2*$^{+/+}$ R1 ES cells; n=5, white bar) does not rescue placental vascularization. In tetraploid *p45NF-E2*$^{+/+}$ control placenta (*p45NF-E2*$^{+/+}$ TA; n=6, black bar) vascularization is normal. Virally mediated tissue-restricted p45NF-E2 expression in the trophectodermal cell lineages rescues placental vascularization in *p45NF-E2*$^{-/-}$ embryos (*p45NF-E2*$^{-/-,+}$ VT; n=6, striped bar) when compared with *p45NF-E2*$^{-/-}$ placentae infected with a control virus (*p45NF-E2*$^{-/-}$ VT; n=6, gray bar). (**E**,**F**) Growth of *p45NF-E2*$^{-/-,+}$ embryos is rescued when compared with *p45NF-E2*$^{+/+}$ control embryos. Bar chart summarizing embryonic length measurements (E; n=6 per group) and representative images of embryos (F). TA, tetraploid aggregation; VT, viral transduction. Mean ± s.e.m. *, P<0.05; **, P<0.01; ANOVA (A-C) or t-test (E). Scale bars: 50 μm in D; 4 mm in F.

Gcm1 mutants lacking Lys387 and Lys426 were generated by site-directed mutagenesis, replacing lysine with arginine residues. Using pLV-Gcm1 as a template, a two-step PCR was conducted with the following primers (5′ to 3′): Gcm1 387K2Rf, ATGCACTGCCCGGCA-GGAGCAACAGGTGG; Gcm1 387K2Rr, CCACCTGTTGCT-CCTGCCGGGCAGTGCAT; Gcm1 426K2Rf, GAGCCTTACGAAGA-GAAGGTATCTGTGGATCTGAGC; and Gcm1 426K2Rr, GCTCAGAT-CCACAGATACCTTCTCTTCGTAAGGCAC. pLV-Gcm1$^{\Delta KK}$ was confirmed by sequencing.

Production of lentiviral particles

VSV-G pseudotyped lentiviral particles were generated as described (Follenzi et al., 2000). Briefly, HEK 293T cells were transfected with pLV-NF-E2, pLV-Gcm1, pLV-Gcm1$^{\Delta KK}$, pLKO1-NF-E2 or pLKO1-Gcm1 together with the packaging plasmid (pCMV-dR8.91) and VSV-G-expressing plasmid (pVSV-G) using the standard calcium phosphate method. Lentiviral particles were harvested 2 and 3 days after transfection and concentrated by ultracentrifugation (50,000 ***g***, 2 hours, twice). After resuspension in Hank's Buffered Salt Solution, the viral particle concentration was determined by measuring p24 tag antigen by ELISA. Viral particles were stored at –80°C.

Transduction of pre-implantation embryos

Two-cell stage embryos were collected at 1.5 dpc and incubated for 2 days to obtain blastocysts. The zona pellucida was removed with acidic Tyrode's solution. Zona pellucida-free embryos were incubated individually in 50 μl KSOM medium containing lentiviral vector (1 μg p24/ml) for 4 hours (Okada et al., 2007). Transduced blastocysts were transferred into pseudopregnant females.

Gene knockdown and knock-in in mouse TS cells

Knockdown of p45NF-E2 or of Gcm1 and knock-in of pLV-Gcm1 in mouse TS cells was performed by lentiviral transduction. pLKO1-NF-E2, pLKO1-Gcm1 or pLV-Gcm1 viral particles were generated as described above. Stable knockdown (p45NF-E2^{kd}) TS cell lines were generated by infecting TS cells with viral particles [5×10^5 transducing units (TU)/ml] in the presence of 8 μg/ml polybrene and 1 μg/ml puromycin. Efficiency of knockdown was assayed by RT-PCR and EMSA in undifferentiated and differentiated TS cells. To generate p45NF-E2/Gcm1 double-knockdown TS cells, p45NF-E2^{kd} cells were transiently infected with pLKO1-Gcm1 shRNA lentiviral particles, yielding p45NF-E2^{kd} Gcm1^{kd} cells. For ectopic expression of Gcm1, TS cells were transiently infected with pLV-Gcm1 lentiviral particles. The efficiency of the Gcm1 knockdown or knock-in was determined after 3 days of differentiation by RT-PCR. In all experiments, cells transduced with non-specific shRNA or pLV-EGFP served as controls.

In vivo HDAC and HAT inhibition

To inhibit HDAC or HAT activity in vivo, pregnant females (*p45NF-E2*$^{+/+}$ for HDAC inhibition, *p45NF-E2*$^{-/-}$ for HAT inhibition) were injected intraperitoneally with the HDAC inhibitor TSA [15 μg/mouse (Nervi et al., 2001)] or valproic acid [sodium salt, 155 mM, 25 ml/kg body weight

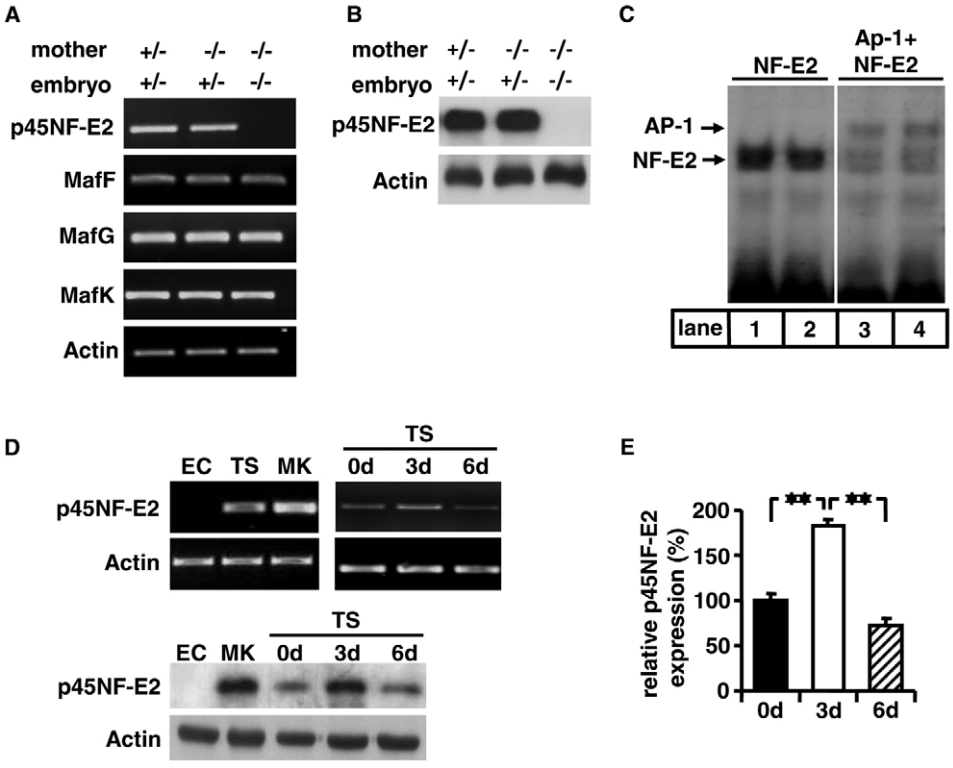

Fig. 2. p45NF-E2 is expressed and differentially regulated in trophoblast cells. (**A**) Expression of the p45 and p18 subunits of NF-E2 in mouse placental tissue (RT-PCR). The genotype refers to *p45NF-E2*. Actin provides a loading control. (**B**) Immunoblotting showing expression of p45NF-E2 in placental tissue. (**C**) Electrophoretic mobility shift assay (EMSA) showing p45NF-E2 binding activity in placental tissue extracts obtained from *p45NF-E2*$^{+/-}$ embryos (14.5 dpc, lanes 1 and 2). Using probes for AP-1 and p45NF-E2 simultaneously, two signals, which correspond to the smaller p45NF-E2 and the larger AP-1 complex, are observed (lanes 3 and 4). (**D**,**E**) Semi-quantitative RT-PCR (D, top) and immunoblot (D, bottom) analyses of p45NF-E2 expression and bar chart summarizing expression relative to day (d) 0 from four independent repeats (E). Murine trophoblast stem (TS) cells, but not murine endothelial cells (ECs; SVEC4-10 cells), express p45NF-E2 (D). Expression of p45NF-E2 is transiently induced during differentiation of murine TS cells at day 3, at which time p45NF-E2 expression is comparable to that in megakaryocytes (MK, D). Mean ± s.e.m. **, $P<0.01$; ANOVA.

(Gottlicher et al., 2001)] or the HAT inhibitor EGCG [50 mg/kg in saline (Giunta et al., 2006)] or curcumin [0.5 mg/kg (Pan et al., 2008)] in 150 µl vehicle [10% (v/v) DMSO in PBS/kg] at 7.5 dpc. The injections were repeated every 48 hours until analysis.

Statistical analysis

In vitro experiments were performed at least in triplicate. Data are expressed as mean ± s.e.m. Statistical analyses were performed using Student's *t*-test or ANOVA. Post-hoc comparisons of ANOVA were corrected using the method of Tukey. Excel (Microsoft, Munich, Germany) and StatistiXL software were used for statistical analyses. Statistical significance was set at $P<0.05$.

RESULTS

Impaired placental vascularization precedes embryonic growth retardation in *p45NF-E2*$^{-/-}$ embryos

We performed timed matings (*p45NF-E2*$^{+/-}$ females × *p45NF-E2*$^{-/-}$ males) to determine the onset of embryonic growth retardation and impaired placental vascularization in *p45NF-E2*$^{-/-}$ embryos (Palumbo et al., 2004; Shivdasani et al., 1995). The growth retardation of *p45NF-E2*$^{-/-}$ embryos first became evident at 16.5 dpc (15.9 mm embryonic length versus 16.6 mm in *p45NF-E2*$^{+/-}$, $P<0.05$) and was readily detectable by 17.5 dpc (16.5 mm versus 19.8 mm, $P<0.001$) (Fig. 1A and see Table S1 in the supplementary material). Impaired vascularization of the placental labyrinthine layer could already be detected at 14.5 dpc (75% vascularization in *p45NF-E2*$^{-/-}$ embryos as compared with 100% in *p45NF-E2*$^{+/-}$ embryos; $P<0.001$; Fig. 1B). The reduction of the vascularized area, as detected by digital image analyses, was associated with reduced placental perfusion (see Fig. S1 in the supplementary material). The manifestation of the IUGR subsequent to the reduced placental vascularization indicates that the IUGR is caused by the placental defect.

Placental expression of p45NF-E2 is required for normal placental vascularization

We next determined whether the placental defect is the consequence of p45NF-E2 deficiency within the embryo proper or within cells of the trophectodermal cell lineage. To achieve p45NF-E2 expression only in the embryo proper and not in the placenta we performed tetraploid aggregation (TA) experiments to generate chimeric embryos derived from *p45NF-E2* wild-type (+/+) embryonic stem (ES) cells and *p45NF-E2*$^{-/-}$ tetraploid embryos. Consistent with p45NF-E2 expression in the embryo proper, *p45NF-E2* mRNA and platelets were readily detectable within the embryo proper (see Fig. S2A in the supplementary material; data not shown). However, vascularization of the labyrinthine layer remained significantly lower than that of control chimeric embryos obtained by fusion of *p45NF-E2*$^{+/+}$ ES cells with *p45NF-E2*$^{+/+}$ tetraploid embryos (76% versus 98%, $P=0.006$; Fig. 1C,D).

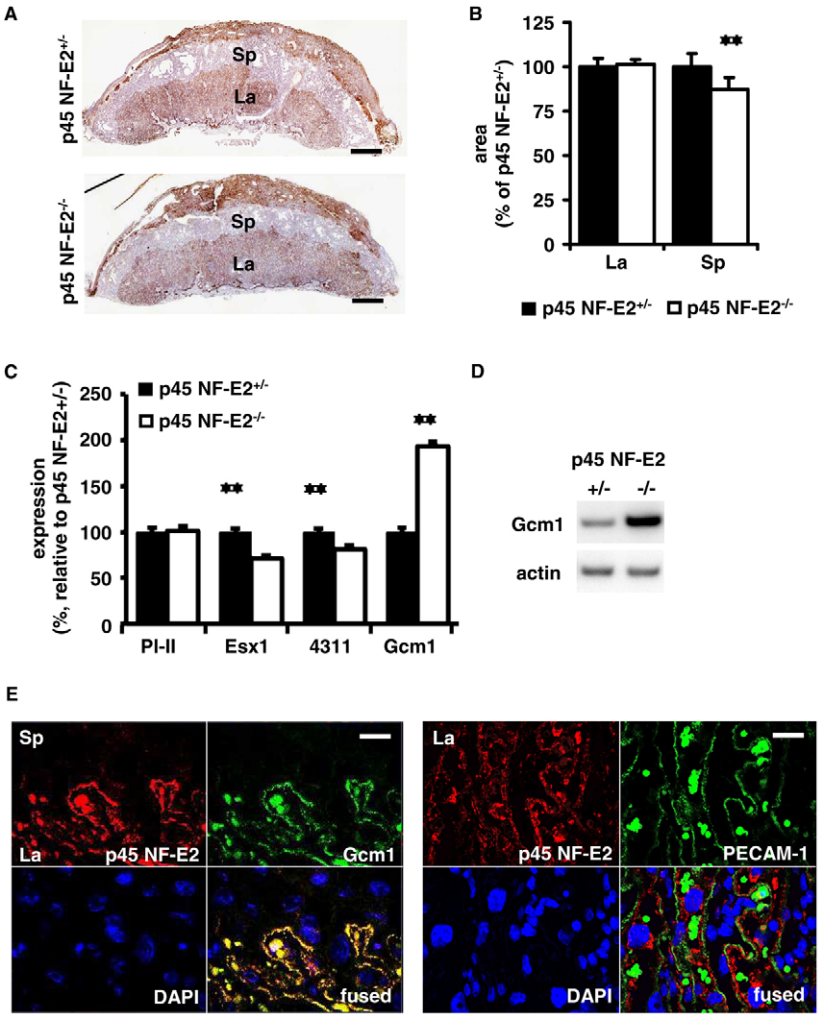

Fig. 3. p45NF-E2 suppresses the expression of Gcm1 in vivo. (**A**,**B**) Analyses of placental morphology in isolectin BS-I B4-stained tissue sections (A) and summary of area measurements (B; $n=8$ per group). The spongiotrophoblast layer (Sp) is slightly reduced, whereas no change in the labyrinthine layer (La) is observed in *p45NF-E2*$^{-/-}$ mice. (**C**,**D**) Bar chart summarizing results of qRT-PCR (C, $n=10$ per group) and Gcm1 immunoblot (D) confirming the marked upregulation of Gcm1 in *p45NF-E2*$^{-/-}$ mouse placental tissue. (**E**) Immunohistochemical analysis of *p45NF-E2*$^{+/-}$ placentae at 14.5 dpc. Expression of p45NF-E2 is detected within the labyrinthine layer and colocalizes with labyrinthine trophoblast cells (Gcm1, left), but not with ECs (Pecam1, right). La, labyrinth; Sp, spongiotrophoblast. Mean ± s.e.m. **, $P<0.01$; ANOVA (B) or *t*-test (C). Scale bars: 500 µm in A; 50 µm in E.

We next restored p45NF-E2 expression specifically within the cells of the trophectodermal lineage by transducing *p45NF-E2*$^{-/-}$ blastocysts with a p45NF-E2-expressing lentivirus (Okada et al., 2007). Following viral transduction (VT) of *p45NF-E2*$^{-/-}$ blastocysts, expression of p45NF-E2 was readily detectable within the placenta, but not within the embryo proper (see Fig. S2B in the supplementary material). Expression of p45NF-E2 within the placenta rescued the vascularization of the labyrinthine layer (99% versus 75%, P=0.004; Fig. 1C,D) and resulted in the normal growth of embryos (weight 98% and length 99% of that of control embryos; Fig. 1E,F). Therefore, expression of p45NF-E2 within trophoblast cells is required for normal placental vascularization and embryonic growth.

p45NF-E2 is expressed in trophoblast cells

Expression of p45NF-E2 was readily detectable in the placental tissue of *p45NF-E2*$^{+/-}$ embryos (Fig. 2A,B). Placental expression of the smaller p18 units of NF-E2 (MafF, MafG, MafK) was independent of embryonic p45NF-E2 expression (Fig. 2A).

The binding activity of p45NF-E2 in 14.5 dpc placental extracts from *p45NF-E2*$^{+/-}$ embryos was readily detectable by EMSA (Fig. 2C, lanes 1 and 2). Placental extracts were co-incubated with radiolabeled probes for activator protein 1 (AP-1) and NF-E2, which share a similar DNA-binding sequence. A slower migrating band, corresponding to the larger AP-1 complex, was clearly observed, demonstrating the specificity of the observed p45NF-E2 signal (Fig. 2C, lanes 3 and 4).

In vitro, p45NF-E2 was expressed in murine trophoblast stem (TS) cells but not in endothelial cells (ECs; SVEC4-10 cells) (Fig. 2D). In differentiating trophoblast cells, expression of p45NF-E2 was transiently induced at day 3 (183% versus 100% at day 0, P=0.002; Fig. 2D,E), at which time p45NF-E2 expression was similar to that in megakaryocytes (Fig. 2D). Thus, p45NF-E2 is expressed in a differentiation-dependent manner in trophoblast cells.

Expression of Gcm1 is enhanced in *p45NF-E2*$^{-/-}$ placentae

The differential expression of p45NF-E2 during trophoblast differentiation raises the question of whether p45NF-E2 itself modulates trophoblast differentiation. Morphometric analyses revealed a small but significant reduction of the spongiotrophoblast layer (88% versus 100% in *p45NF-E2*$^{+/-}$ placentae, P=0.0028; Fig. 3A,B) and in the expression of the spongiotrophoblast marker *4311* (*Tpbpa* – Mouse Genome Informatics) (86%, P=0.007; Fig. 3C) in *p45NF-E2*$^{-/-}$ placentae. The area of the labyrinthine layer did not differ between *p45NF-E2*$^{-/-}$ and *p45NF-E2*$^{+/-}$ embryos (101% versus 100%, P=0.84; Fig. 3A,B). Interestingly, expression of the labyrinthine layer marker *Esx1* was slightly reduced (76%, P=0.004; Fig. 3C), whereas expression of the syncytiotrophoblast marker Gcm1 was markedly increased (193%, P=0.001; Fig. 3C,D). Expression of the giant trophoblast marker placenta lactogen II (*Pl-ll*; *Prl3b1* – Mouse Genome Informatics) did not differ between *p45NF-E2*$^{-/-}$ and *p45NF-E2*$^{+/-}$ embryos (Fig. 3C). Expression of p45NF-E2 colocalized with that of Gcm1 but not with the EC marker Pecam1 in the labyrinthine layer of the placenta (Fig. 3E and see Fig. S3 in the supplementary material).

p45NF-E2 regulates syncytiotrophoblast formation in vivo

To determine the consequences of p45NF-E2 deficiency for syncytiotrophoblast morphology in vivo, we performed ultrastructural analyses. Evaluation of transmission electron

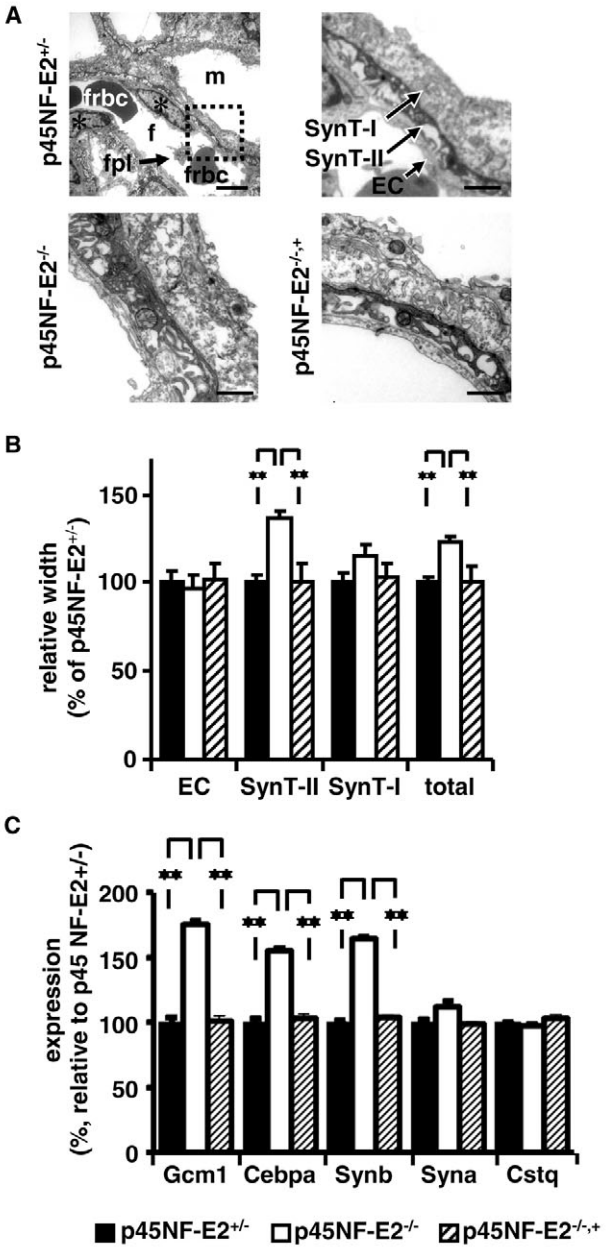

Fig. 4. Increased syncytiotrophoblast width in *p45NF-E2*$^{-/-}$ placentae. (**A**,**B**) Electron microscopy (EM) analyses of syncytiotrophoblasts in placentae from *p45NF-E2*$^{+/-}$, *p45NF-E2*$^{-/-}$ or *p45NF-E2*$^{-/-}$ mouse embryos with trophectodermal-specific expression of p45NF-E2 (*p45NF-E2*$^{-/-,+}$). (A) Overview image (top left) of the placental labyrinthine layer of a *p45NF-E2*$^{+/-}$ embryo showing fetal red blood cells (frbc), a fetal platelet (fpl) and the nuclei of embryonic ECs (asterisks). The boxed area is shown at high magnification to the right, showing the trilaminar trophoblast structure that separates the maternal and fetal blood compartments. In *p45NF-E2*$^{-/-}$ (bottom left) but not *p45NF-E2*$^{-/-,+}$ (bottom right) placentae, the width of syncytiotrophoblast layer 2 (SynT-II) and the total width of the maternal-embryonic barrier are significantly increased. Fetal (f) and maternal (m) blood space; SynT-I, syncytiotrophoblast layer 1; EC, endothelial cell layer. (B) Bar chart summarizing the results of the EM analyses (n=6 per group; ≥30 images per placenta). (**C**) qRT-PCR analysis showing that expression of *Gcm1*, *Cebpa* and *Synb* is increased in *p45NF-E2*$^{-/-}$ placentae (as compared with *p45NF-E2*$^{+/-}$ controls) and is rescued in *p45NF-E2*$^{-/-,+}$ placentae. n=6 per group. Total, total width of the embryonic maternal barrier. Mean ± s.e.m. **, P<0.01; ANOVA. Scale bars: 1 μm.

microscopy images showed an increased width of the total maternal-embryonic barrier in *p45NF-E2*$^{-/-}$ embryos as compared with *p45NF-E2*$^{+/-}$ littermates at 16.5 dpc (121% versus 100% in *p45NF-E2*$^{+/-}$, P=0.004; Fig. 4A,B). Detailed morphological analyses revealed thickening of syncytiotrophoblast layer 2 (SynT-II) in *p45NF-E2*$^{-/-}$ embryos (136%, P<0.001; Fig. 4A,B). No obvious alteration of ECs or mononuclear sinusoidal trophoblast giant cells was detected. Consistent with the increased width of SynT-II, the expression of Gcm1 and of the Gcm1-dependent genes *Cebpa* and *Synb* (D930020E02Rik – Mouse Genome Informatics) (Fig. 4C), which are markers of SynT-II (Simmons et al., 2008a), was significantly increased. Expression of *Syna* (*Gm52* – Mouse Genome Informatics), which is not expressed in SynT-II, or of *Ctsq*, a marker of sinusoidal giant trophoblast cells, was not altered (Fig. 4C). Lentiviral-mediated reconstitution of p45NF-E2 expression in trophectodermal cells of *p45NF-E2*$^{-/-}$ embryos (*p45NF-E2*$^{-/-,+}$) rescued the width of the syncytiotrophoblast layers and the expression of *Gcm1*, *Cepba* and *Synb* (Fig. 4A-C). The absence of the transcription factor p45NF-E2 from trophoblast cells therefore enhances the width of SynT-II.

Reduction of p45NF-E2 expression enhances syncytium formation in vitro via Gcm1

To determine whether p45NF-E2 modulates syncytium formation cell-autonomously, we performed in vitro experiments employing p45NF-E2 knockdown (p45NF-E2^{kd}) trophoblast cells. The expression and binding activity of *p45NF-E2* mRNA were significantly reduced in p45NF-E2^{kd} cells (see Fig. S4 in the supplementary material). Differentiation of p45NF-E2^{kd} cells for 6 days resulted in enhanced syncytiotrophoblast formation [average number of trophoblast syncytia per random image: 2.7 versus 0.5 in control (p45NF-E2^{c}) cells, P=0.005; Fig. 5A,B]. Consistent with the enhanced syncytium formation, the expression of the syncytiotrophoblast markers *Gcm1* (193%, P=0.002), *Cebpa* (163%, P=0.008) and *Synb* (176%, P=0.004) (Fig. 5C,D) was markedly increased.

We next determined whether p45NF-E2-dependent regulation of Gcm1 expression is mechanistically linked with altered syncytiotrophoblast formation. Lentiviral-mediated overexpression of Gcm1 in control TS cells increased syncytiotrophoblast formation (2.2 in p45NF-E2^{c} Gcm1^{+} cells versus 0.5 in p45NF-E2^{c} cells, P=0.007; Fig. 5A,B) and expression of the Gcm1-dependent genes *Cebpa* (175%, P=0.004) and *Synb* (184%, P=0.004) (Fig. 5C,D) after 6 days of differentiation. Thus, increased expression of Gcm1 is sufficient to enhance syncytiotrophoblast formation in vitro.

To determine whether increased Gcm1 expression is required for the enhanced syncytiotrophoblast formation in p45NF-E2-deficient trophoblast cells, we reduced the expression of Gcm1 in p45NF-E2^{kd} TS cells. This rescued syncytiotrophoblast formation (0.4 in p45NF-E2^{kd} Gcm1^{kd} cells versus 2.7 in p45NF-E2^{kd} control cells, P<0.001; Fig. 5A,B) and reduced the expression of *Cebpa* (27%, P<0.001) and *Synb* (25%, P<0.001) (Fig. 5C,D) after 6 days of differentiation. These results establish that p45NF-E2 cell-autonomously represses Gcm1, preventing excess syncytiotrophoblast formation.

p45NF-E2 regulates acetylation of Gcm1

The transcriptional activity of Gcm1 is increased by CBP (Crebbp – Mouse Genome Informatics)-dependent acetylation (Chang et al., 2005). Since p45NF-E2 interacts with CBP, which regulates

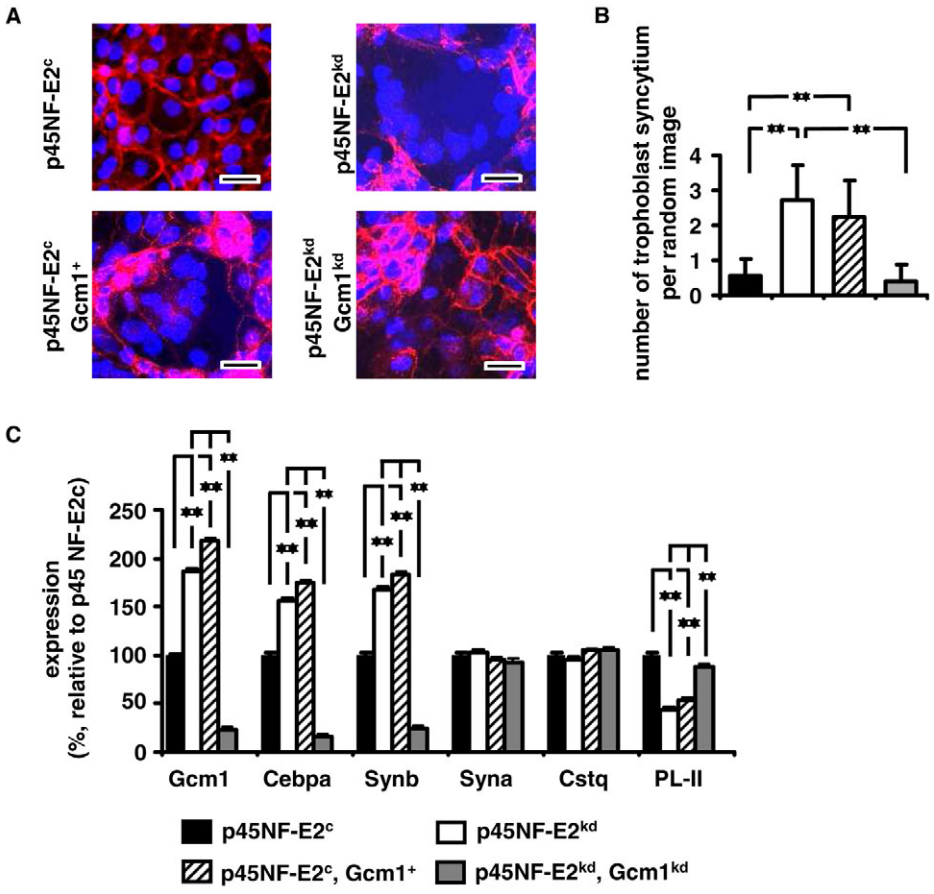

Fig. 5. The enhanced syncytiotrophoblast formation in p45NF-E2-deficient trophoblast cells is Gcm1 dependent. (**A**,**B**) Overexpression of Gcm1 (p45NF-E2^{c} Gcm1^{+}) increases syncytiotrophoblast formation. Reduction of Gcm1 expression in p45NF-E2-deficient mouse cells (p45NF-E2^{kd} Gcm1^{kd}) reduces syncytiotrophoblast formation to the levels observed in control (p45NF-E2^{c}) trophoblast cells. (A) Six-day-differentiated trophoblast cells were stained with CellMask (red) and counterstained with DAPI (blue). Scale bars: 20 μm (B) Bar chart summarizing the results of syncytiotrophoblast quantitation from three independent experiments (≥30 random images per group). (**C**) Expression analyses (qRT-PCR) of *Gcm1*, *Cebpa* and *Synb* in trophoblast cells (three independent repeat experiments). p45NF-E2^{c}, control transfected trophoblast cells; p45NF-E2^{c} Gcm1^{+}, Gcm1-overexpressing trophoblast cells; p45NF-E2^{kd}, p45NF-E2 knockdown trophoblast cells; p45NF-E2^{kd} Gcm1^{kd}, p45NF-E2 and Gcm1 double-knockdown trophoblast cells. Mean ± s.e.m. **, P<0.01; ANOVA.

acetylation in mouse erythroleukemia (MEL) cells (Kiekhaefer et al., 2004), we explored whether p45NF-E2 regulates Gcm1 via acetylation.

First, we evaluated whether p45NF-E2 modulates the CBP-Gcm1 interaction. Using immunoprecipitation we detected only a weak CBP-Gcm1 interaction in the presence of p45NF-E2, whereas a strong CBP-Gcm1 interaction was observed in the absence of p45NF-E2 (Fig. 6A). As expected, no p45NF-E2 could be detected in the immunoprecipitates of p45NF-E2-deficient tissues or cells (Fig. 6A). However, in tissue extracts from *p45NF-E2*$^{+/-}$ placentae or p45NF-E2 control trophoblast cells, p45NF-E2 strongly co-immunoprecipitated with CBP (Fig. 6A). Thus, in the absence of p45NF-E2, the interaction of Gcm1 with CBP, which possesses an intrinsic acetyltransferase activity, is increased.

Immunoprecipitation experiments revealed increased acetylation of Gcm1 in *p45NF-E2*$^{-/-}$ placentae and in p45NF-E2^{kd} trophoblast cells [149% compared with *p45NF-E2*$^{+/-}$ placentae (P=0.002) and 137% compared with p45NF-E2-expressing control cells (P=0.005), respectively; Fig. 6B,C]. Hence, p45NF-E2 modifies Gcm1 post-translationally via acetylation. Furthermore, acetylation of histone H4 (ac-H4) within the *Gcm1* promoter was enhanced in *p45NF-E2*$^{-/-}$ placentae or p45NF-E2^{kd} trophoblast cells [187% (P=0.006) and 169% (P=0.008), respectively; Fig. 6D,E], implying that p45NF-E2 in addition epigenetically regulates Gcm1 expression via acetylation.

p45NF-E2 modulates syncytiotrophoblast formation via acetylation

Compared with p45NF-E2-expressing trophoblast control cells (p45NF-E2^{c}), histone deacetylase (HDAC) activity was reduced to 68% in p45NF-E2^{kd} cells (P=0.03; Fig. 7A). To determine the mechanistic relevance of altered acetylation we modulated acetylation in p45NF-E2^{c} and p45NF-E2^{kd} trophoblast cells in vitro. Treatment of p45NF-E2^{c} trophoblast cells with the HDAC inhibitor TSA reduced HDAC activity to 62% (versus untreated p45NF-E2^{c} cells, P=0.01; Fig. 7A). HDAC inhibition with TSA enhanced syncytium formation (2.7 versus 0.5 in p45NF-E2^{c} cells, P=0.004; Fig. 7B,C) and the expression of syncytiotrophoblast markers (Gcm1, Cebpa, Synb) significantly (Fig. 7D).

Conversely, the histone acetyltransferase (HAT) inhibitor curcumin rescued HDAC activity in p45NF-E2^{kd} trophoblast cells (107% versus P45NF-E2^{kd}, P=0.006; Fig. 7A). HAT inhibition using curcumin reduced syncytium formation (0.7 versus 2.7 in untreated p45NF-E2^{kd} cells, P=0.009; Fig. 7B,C) and decreased the expression of syncytiotrophoblast markers (Gcm1, Cebpa, Synb) in p45NF-E2^{kd} cells (Fig. 7D). Similar results were obtained using the HAT inhibitor EGCG (Giunta et al., 2006) (data not shown). Thus, enhanced syncytiotrophoblast formation in p45NF-E2-deficient trophoblast cells is acetylation dependent.

Previous data established that the transcriptional activity of human GCM1 is enhanced by acetylation of lysine residues (Chang et al., 2005). To determine whether post-translational

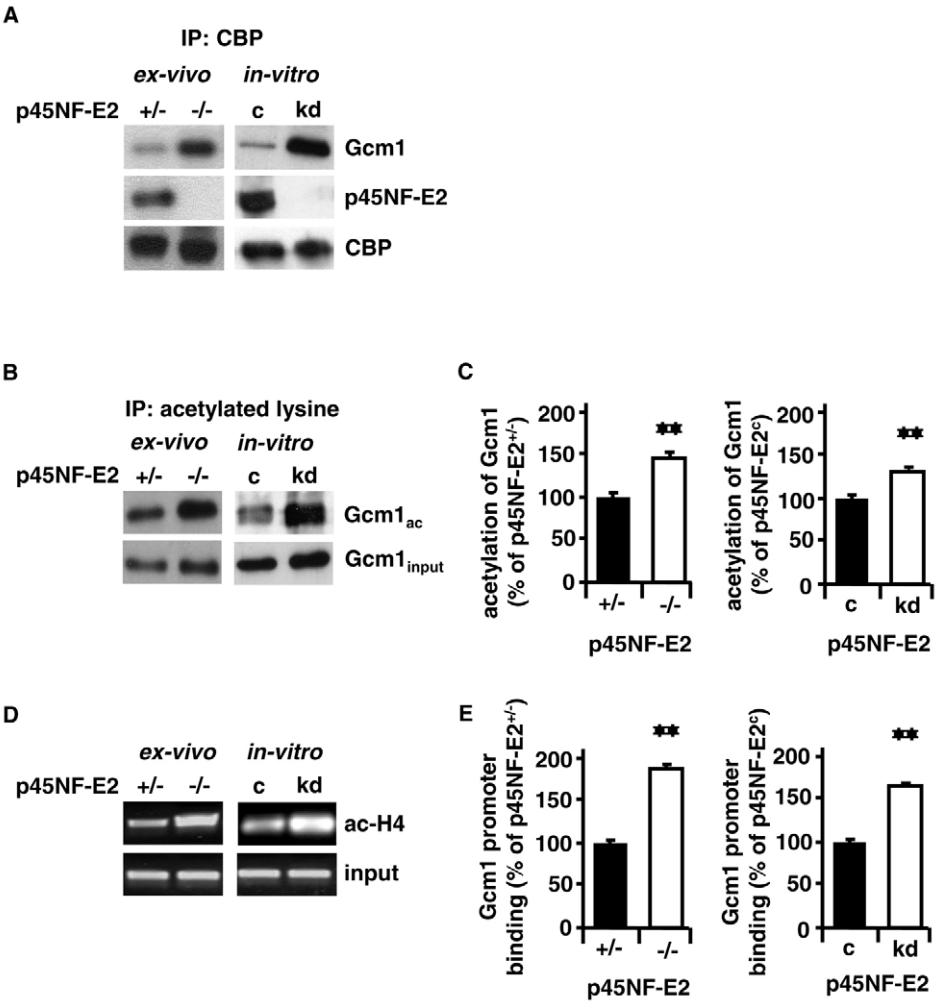

Fig. 6. Increased acetylation at the *Gcm1* promoter and of Gcm1 protein in the absence of p45NF-E2. (**A**) p45NF-E2 inhibits the interaction of CBP with Gcm1. Immunoprecipitation of CBP followed by immunoblotting of p45NF-E2, Gcm1 or CBP. (**B**,**C**) Increased lysine acetylation of Gcm1 in p45NF-E2-deficient mouse placentae (*p45NF-E2*$^{-/-}$) or trophoblast cells (p45NF-E2^{kd}). (B) Increased acetylation of Gcm1 in the absence of p45NF-E2. Immunoprecipitation using an antibody against acetylated lysine followed by immunoblotting of Gcm1 (top, Gcm1$_{ac}$) and immunoblotting of Gcm1 without prior immunoprecipitation (bottom, Gcm1$_{input}$). (C) The average levels of acetylated Gcm1 (normalized to Gcm1$_{input}$). (**D**,**E**) Acetylation of histone H4 within the *Gcm1* promoter is enhanced in *p45NF-E2*$^{-/-}$ placentae and p45NF-E2^{kd} trophoblast cells. (D) Semi-quantitative PCR of the *Gcm1* promoter after chromatin immunoprecipitation using an antibody against acetylated histone H4 (ac-H4). (E) Summary of the ChIP assay results from placental extracts (ex vivo, n=6; left) or in vitro experiments (n≥4; right). IP, immunoprecipitation; c, control trophoblast cells; kd, p45NF-E2 knockdown trophoblast cells. Mean ± s.e.m. **, P<0.01; t-test.

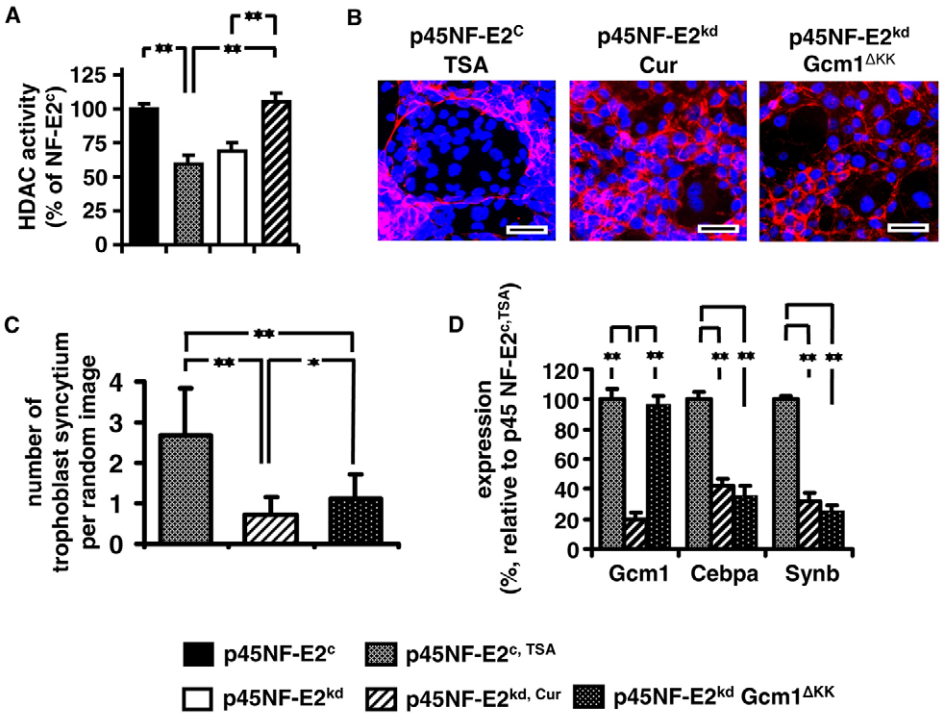

Fig. 7. p45NF-E2 regulates syncytiotrophoblast formation via acetylation. (**A**) Histone deacetylase (HDAC) activity is reduced in p45NF-E2^{kd} mouse trophoblast cells. Inhibition of HDAC using TSA reduces HDAC activity in p45NF-E2^{c} trophoblast cells, whereas the histone acetyltransferase (HAT) inhibitor curcumin (Cur) enhances HDAC activity in p45NF-E2^{kd} trophoblast cells (three repeat experiments). (**B**,**C**) Inhibition of HDAC activity in p45NF-E2-expressing cells (p45NF-E2^{c} TSA) increases syncytiotrophoblast formation, whereas treatment with curcumin (p45NF-E2^{kd} Cur) or transfection with the Gcm1$^{\Delta KK}$ mutant decreases syncytiotrophoblast formation in p45NF-E2-deficient cells. (B) Six-day-differentiated trophoblast cells were stained with CellMask and counterstained with DAPI. (C) Summary of the syncytiotrophoblast quantitation results (≥30 random images per group; three independent repeat experiments). (**D**) Expression of syncytiotrophoblast markers (*Gcm1*, *Cebpa*, *Synb*), as assessed by qRT-PCR, following modulation of acetylation in vitro (three independent repeat experiments). Mean ± s.e.m. *, P<0.05; **, P<0.01; ANOVA. Scale bars: 200 μm.

modification of Gcm1 via acetylation contributes to enhanced syncytiotrophoblast formation we replaced two lysine residues of murine Gcm1 with arginine (Gcm1$^{\Delta KK}$). Following lentiviral-mediated transient transfection of p45NF-E2^{kd} cells with Gcm1$^{\Delta KK}$, acetylation of Gcm1 was markedly reduced (as determined by immunoprecipitation, data not shown). In p45NF-E2^{kd} Gcm1$^{\Delta KK}$ trophoblast cells, syncytiotrophoblast formation was markedly reduced (1.1 versus 2.7 in p45NF-E2^{kd} cells, P<0.001; Fig. 7B,C). However, syncytiotrophoblast formation remained slightly higher than in curcumin-treated p45NF-E2^{kd} cells (1.1 versus 0.7 in p45NF-E2^{kd} cells, P=0.010; Fig. 7B,C). Concomitantly, we observed a reduction in expression of the Gcm1-dependent genes *Cebpa* (36%, P<0.001) and *Synb* (25%, P<0.001) in Gcm1$^{\Delta KK}$-transfected p45NF-E2^{kd} cells (Fig. 7D). These data establish that the increased syncytiotrophoblast formation in p45NF-E2-deficient trophoblast cells depends largely on post-translational modification of Gcm1 by acetylation. However, other effects, such as the acetylation of other proteins and epigenetic gene regulation via acetylation, might contribute to the enhanced syncytiotrophoblast formation in p45NF-E2-deficient trophoblast cells.

p45NF-E2 modulates syncytiotrophoblast formation and placental vascularization via acetylation in vivo

Injection of HDAC inhibitors (TSA or valproic acid) into pregnant *p45NF-E2*$^{+/+}$ mice mated with *p45NF-E2*$^{+/+}$ males reduced HDAC activity and increased acetylation within the placenta (53%, P=0.004; Fig. 8A and data not shown). In utero exposure of *p45NF-E2*$^{+/+}$ embryos to HDAC inhibitors impaired placental vascularization [73% in *p45NF-E2*$^{+/+}$ TSA-treated embryos versus 100% in untreated *p45NF-E2*$^{+/+}$ control (*p45NF-E2*$^{+/+c}$) embryos, P=0.007; Fig. 8B,C], impaired embryonic growth [weight, 72% (P<0.017); length, 93% (P<0.021) compared with *p45NF-E2*$^{+/+c}$ embryos] and increased the width of SynT-II (145%, P<0.001; Fig. 8D,E). The expression of the syncytiotrophoblast markers *Gcm1* (172%), *Cebpa* (145%) and *Synb* (163%) was induced to a comparable extent as in *p45NF-E2*$^{-/-}$ control (*p45NF-E2*$^{-/-c}$) placental tissues (Fig. 8F).

Conversely, treatment of pregnant mice carrying *p45NF-E2*$^{-/-}$ embryos with HAT inhibitors (curcumin or EGCG) increased HDAC activity and reduced protein acetylation (Fig. 8A and data not shown). Following HAT inhibition, placental vascularization (98% versus 100% in *p45NF-E2*$^{+/+c}$ mice, P=0.96; Fig. 8B,C), embryonic growth [weight, 97% (P=0.86); length, 98% (P=0.79)] and the width of SynT-II (98%, P=0.58; Fig. 8D,E) were rescued in *p45NF-E2*$^{-/-}$ embryos (*p45NF-E2*$^{-/-}$ Cur). Furthermore, the expression of the syncytiotrophoblast markers *Gcm1* (103%), *Cebpa* (97%) and *Synb* (109%) was rescued (Fig. 8F).

The reversibility of reduced placental vascularization, impaired embryonic growth, enhanced syncytiotrophoblast formation and increased expression of *Gcm1*, *Cebpa* and *Synb* in *p45NF-E2*$^{-/-}$ placentae or trophoblast cells upon inhibition of acetylation establishes that the placental and trophoblast differentiation defects in *p45NF-E2*$^{-/-}$ embryos are mechanistically linked to altered acetylation activity.

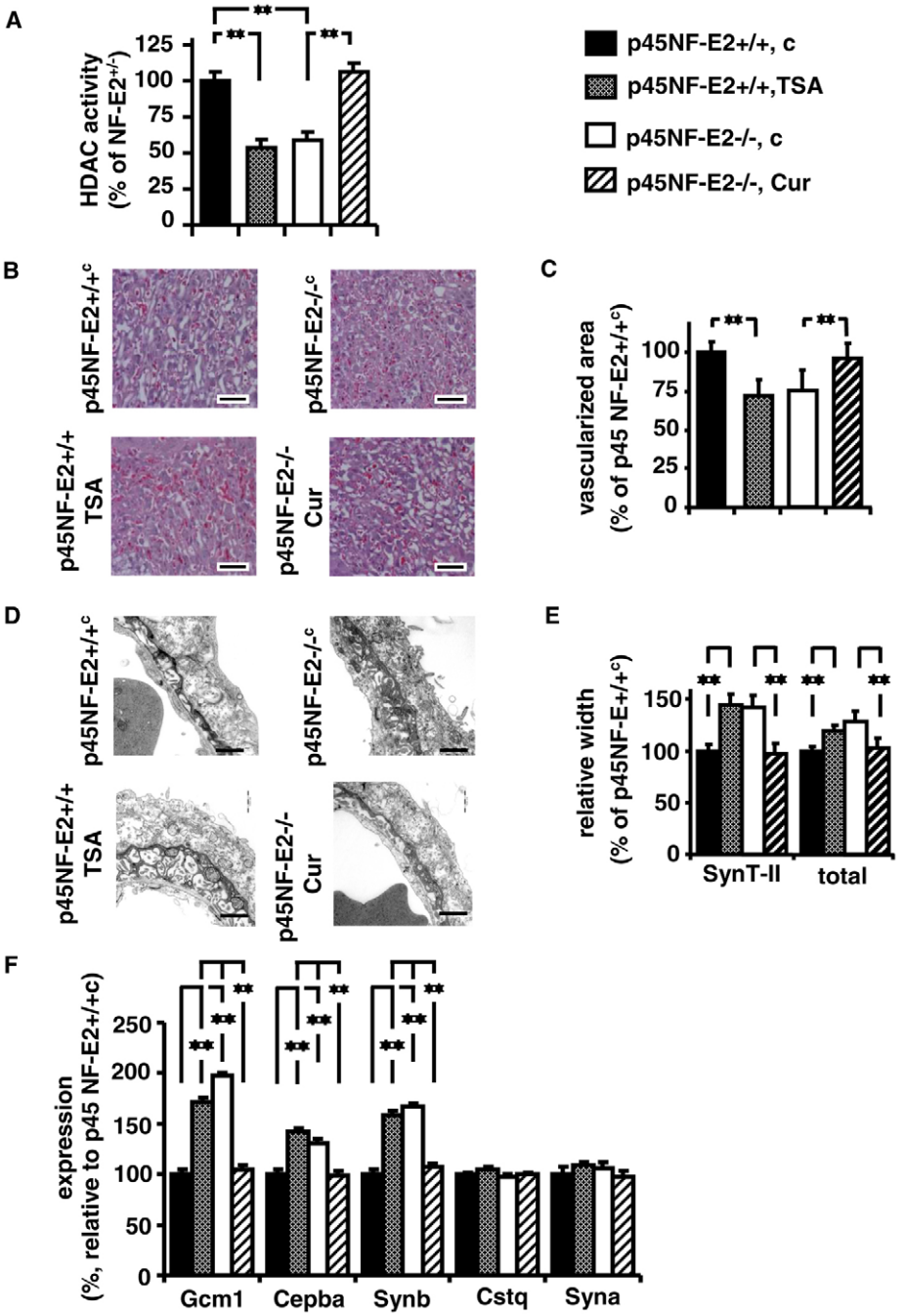

Fig. 8. p45NF-E2 regulates syncytiotrophoblast differentiation and placental vascularization via acetylation in vivo. (**A**) HDAC activity is reduced in placental extracts from *p45NF-E2*$^{-/-c}$ (untreated control) mouse embryos as compared with tissue extracts from p45NF-E2-expressing placentae (*p45NF-E2*$^{+/+c}$). In vivo intervention with TSA reduces HDAC activity in p45NF-E2-expressing placentae (*p45NF-E2*$^{+/+}$ TSA), whereas curcumin increases HDAC activity in *p45NF-E2*$^{-/-}$ placentae (*p45NF-E2*$^{-/-}$ Cur). (**B**,**C**) Inhibition of HDAC activity impairs placental vascularization in *p45NF-E2*$^{+/+}$ placentae (*p45NF-E2*$^{+/+}$ TSA). Restoring HDAC activity in *p45NF-E2*$^{-/-}$ placentae using curcumin (*p45NF-E2*$^{-/-}$ Cur) rescues placental vascularization. (B) HE-stained placental sections. (C) Summary of vascularization measurements ($n \geq 5$ per group). (**D**,**E**) In utero exposure of wild-type embryos to TSA (*p45NF-E2*$^{+/+}$ TSA) increases the width of SynT-II and the total width of the embryonic-maternal barrier (total). Inhibition of acetylation in *p45NF-E2*$^{-/-}$ embryos using curcumin (*p45NF-E2*$^{-/-}$ Cur) rescues the width of SynT-II and of the placental embryonic-maternal barrier. (D) Representative electron microscopy images. (E) Summary of relative width measurements ($n \geq 5$ per group, ≥30 images per placenta). (**F**) Expression (qRT-PCR) of syncytiotrophoblast markers (*Gcm1*, *Cebpa*, *Synb*) following in utero modulation of HDAC activity ($n \geq 5$ per group). Mean ± s.e.m. **, $P<0.01$; ANOVA. Scale bars: 50 μm in B; 1 μm in D.

DISCUSSION

The present study identifies a novel mechanism regulating syncytium formation of trophoblast cells. The transcription factor p45NF-E2, which hitherto was thought to be specific to hematopoietic cells, cell-autonomously represses Gcm1-dependent syncytium formation in trophoblast cells. This interaction of p45NF-E2 and Gcm1 depends, in vitro and in vivo, on acetylation, establishing that acetylation is crucial for syncytiotrophoblast formation, placental function and embryonic growth.

Hitherto, *p45NF-E2*$^{-/-}$ mice were best known for their megakaryocyte maturation defect, which results in thrombocytopenia (Shivdasani et al., 1995). We now demonstrate that the placental defect and the IUGR of *p45NF-E2*$^{-/-}$ embryos are independent of thrombocytopenia. This establishes that embryonic platelets and platelet-released mediators are dispensable for embryonic and placental development. This provides conclusive evidence that the developmental function of the embryonic hemostatic system is independent of the primary endpoint of hemostasis (the interaction of fibrin and platelets). The lethal embryonic phenotypes of embryos lacking some coagulation factors (e.g. tissue factor, prothrombin, factor X) must therefore be caused by mechanisms that are independent of the fibrin-platelet interaction and instead most likely related to the developmental function of PAR proteins in vascular and non-vascular tissues (Bugge et al., 1996; Camerer et al., 2010; Carmeliet et al., 1996; Cui et al., 1996; Griffin et al., 2001; Sun et al., 1998; Toomey et al., 1996; Xue et al., 1998).

The current study identifies a novel developmental function of p45NF-E2 in non-hematopoietic cells. Unlike in hematopoietic cells, where p45NF-E2 is perceived as a positive regulator (Andrews, 1998), p45NF-E2 must act as a repressor during syncytiotrophoblast development as the absence of p45NF-E2 enhances the expression of Gcm1 and of Gcm1-dependent genes and promotes syncytiotrophoblast formation. Considering the distinct functions of p45NF-E2 during the development of hematopoietic cells (transcriptional activation) and trophoblast cells (transcriptional repression), we propose that p45NF-E2 modulates hematopoietic and trophoblast cell differentiation through at least partially diverse mechanisms.

The mechanism through which p45NF-E2 governs megakaryocyte maturation remains incompletely understood. Of note, treatment of patients with HDAC inhibitors results in thrombocytopenia (Prince et al., 2009) and combined Hdac1 and Hdac2 deficiency results in megakaryocyte apoptosis and thrombocytopenia in mice (Wilting et al., 2010). Although it remains unknown whether the thrombocytopenia observed in p45NF-E2-deficient mice is related to altered acetylation, we establish that the placental phenotype and IUGR of *p45NF-E2*$^{-/-}$ embryos are mechanistically linked to acetylation-dependent syncytiotrophoblast differentiation. This role of acetylation in trophoblast cells is in agreement with the acetylation-dependent syncytiotrophoblast formation in aryl hydrocarbon receptor nuclear translocator (Arnt, or Hif1β)-deficient trophoblast cells in vitro (Maltepe et al., 2005). The activity of HDACs, which are also referred to as lysine deacetylases (KDACs) or protein deacetylases (PDACs), was reduced in the absence of p45NF-E2. Enhanced acetylation was not specific for Gcm1, as we consistently observed a general increase in protein acetylation (data not shown). Indeed, in addition to the post-translational modification of Gcm1, we observed enhanced histone H4 acetylation within the *Gcm1* promoter and increased *Gcm1* mRNA levels in p45NF-E2-deficient trophoblast cells, indicating that p45NF-E2 regulates Gcm1 both epigenetically and post-translationally. Furthermore, it is possible that the post-translational modification of proteins other than Gcm1 contributes to the p45NF-E2-dependent placental phenotype. However, given the well-established pivotal role of Gcm1 in labyrinthine layer formation (Anson-Cartwright et al., 2000) and the current data showing that overexpression of Gcm1 is sufficient to increase syncytiotrophoblast formation, we conclude that enhanced expression of Gcm1 is crucial for the increased syncytiotrophoblast formation and the placental defect observed in *p45NF-E2*$^{-/-}$ embryos.

The enhanced Gcm1 acetylation observed in the absence of p45NF-E2 is associated with the increased expression of Gcm1-dependent genes (*Cebpa* and *Synb*) relevant to murine syncytiotrophoblast formation (Simmons et al., 2008b). This is in agreement with findings in human trophoblast cells showing that acetylation increases the stability of GCM1 and the binding of GCM1 to the promoter of the syncytin (*ERVWE1* – Human Gene Nomenclature Committee) gene, which encodes a placental fusogenic membrane protein (Chang et al., 2005; Chuang et al., 2006).

The transcription factor Gcm1 has two functions during placentation. It is required for (1) the initial folding of the chorion into simple branches and the subsequent branching morphogenesis within the placental labyrinthine layer and (2) syncytiotrophoblast fusion (Anson-Cartwright et al., 2000). Although, in the absence of Gcm1, both branching and syncytiotrophoblast fusion are impaired resulting in embryonic lethality at E10.5 (Anson-Cartwright et al., 2000; Schreiber et al., 2000a), overexpression of Gcm1 in *p45NF-E2*$^{-/-}$ placenta has no apparent impact on EC or gross branching morphology. Thus, chorioallantoic fusion, embryonic EC invasion and chorioallantoic branching appear to be unaffected by high levels of Gcm1 expression in *p45NF-E2*$^{-/-}$ placentae. The observed thickening of SynT-II in *p45NF-E2*$^{-/-}$ placentae with high-level Gcm1 expression reflects a terminal syncytiotrophoblast differentiation defect during placental labyrinthine formation, resulting in a milder, non-lethal phenotype at a later stage. The different phenotypes that result from reduced or increased Gcm1 expression indicate that the two Gcm1-dependent effects are controlled through partially distinct mechanisms during placentation.

The enhanced Gcm1 expression and syncytiotrophoblast formation observed in murine p45NF-E2-deficient placentae and trophoblast cells might be of pathophysiological relevance to placental dysfunction in humans, as we have observed p45NF-E2 expression in human placental tissues (M.K. and B.I., unpublished) and because altering GCM1 expression triggers parallel changes in human trophoblast cells (Baczyk et al., 2009) to those observed in mice. Interestingly, both increased and decreased GCM1 expression have been reported in human placenta obtained from complicated pregnancies (Chen et al., 2004; Fujito et al., 2006; McCaig and Lyall, 2009). The placental defects associated with either the loss or gain of Gcm1 function observed in mice (Anson-Cartwright et al., 2000) (this paper) provide a rationale for the apparently paradoxical findings of the aforementioned clinical studies. The current results might aid in deciphering the mechanisms that result in placental dysfunction associated with low or high levels of GCM1 expression in humans.

Acknowledgements

P45NF-E2-deficient mice were kindly provided by R. Shivdasani (Harvard Medical School, Cambridge, MA, USA). We thank S. Schmidt and F. Zimmermann for technical support; and Hilmar Bading, Department of Neurobiology, Interdisciplinary Center for Neurosciences, University of Heidelberg, for providing the opportunity to carry out the electron microscopy work in his laboratory. This work was supported by grants of the Deutsche Forschungsgemeinschaft (IS 67/4-1, IS 67/4-2) to B.I. and a grant of the German Israeli foundation to B.I. and P.P.N. K.S. has a scholarship from the DAAD.

Competing interests statement

The authors declare no competing financial interests.

Supplementary material

Supplementary material for this article is available at
http://dev.biologists.org/lookup/suppl/doi:10.1242/dev.059105/-/DC1

References

Andrews, N. C. (1998). The NF-E2 transcription factor. *Int. J. Biochem. Cell Biol.* **30**, 429-432.

Anson-Cartwright, L., Dawson, K., Holmyard, D., Fisher, S. J., Lazzarini, R. A. and Cross, J. C. (2000). The glial cells missing-1 protein is essential for branching morphogenesis in the chorioallantoic placenta. *Nat. Genet.* **25**, 311-314.

Baczyk, D., Drewlo, S., Proctor, L., Dunk, C., Lye, S. and Kingdom, J. (2009). Glial cell missing-1 transcription factor is required for the differentiation of the human trophoblast. *Cell Death Differ.* **16**, 719-727.

Balasubramanyam, K., Varier, R. A., Altaf, M., Swaminathan, V., Siddappa, N. B., Ranga, U. and Kundu, T. K. (2004). Curcumin, a novel p300/CREB-binding protein-specific inhibitor of acetyltransferase, represses the acetylation of histone/nonhistone proteins and histone acetyltransferase-dependent chromatin transcription. *J. Biol. Chem.* **279**, 51163-51171.

Bierhaus, A., Schiekofer, S., Schwaninger, M., Andrassy, M., Humpert, P. M., Chen, J., Hong, M., Luther, T., Henle, T., Kloting, I. et al. (2001). Diabetes-associated sustained activation of the transcription factor nuclear factor-kappaB. *Diabetes* **50**, 2792-2808.

Brenner, B. and Kupferminc, M. J. (2003). Inherited thrombophilia and poor pregnancy outcome. *Best Pract. Res. Clin. Obstet. Gynaecol.* **17**, 427-439.

Bugge, T. H., Xiao, Q., Kombrinck, K. W., Flick, M. J., Holmback, K., Danton, M. J., Colbert, M. C., Witte, D. P., Fujikawa, K., Davie, E. W. et al. (1996). Fatal embryonic bleeding events in mice lacking tissue factor, the cell-associated initiator of blood coagulation. *Proc. Natl. Acad. Sci. USA* **93**, 6258-6263.

Camerer, E., Duong, D. N., Hamilton, J. R. and Coughlin, S. R. (2004). Combined deficiency of protease-activated receptor-4 and fibrinogen recapitulates the hemostatic defect but not the embryonic lethality of prothrombin deficiency. *Blood* **103**, 152-154.

Camerer, E., Barker, A., Duong, D. N., Ganesan, R., Kataoka, H., Cornelissen, I., Darragh, M. R., Hussain, A., Zheng, Y. W., Srinivasan, Y. et al. (2010). Local protease signaling contributes to neural tube closure in the mouse embryo. *Dev. Cell* **18**, 25-38.

Carmeliet, P., Ferreira, V., Breier, G., Pollefeyt, S., Kieckens, L., Gertsenstein, M., Fahrig, M., Vandenhoeck, A., Harpal, K., Eberhardt, C. et al. (1996). Abnormal blood vessel development and lethality in embryos lacking a single VEGF allele. *Nature* **380**, 435-439.

Chang, C. W., Chuang, H. C., Yu, C., Yao, T. P. and Chen, H. (2005). Stimulation of GCMa transcriptional activity by cyclic AMP/protein kinase A signaling is attributed to CBP-mediated acetylation of GCMa. *Mol. Cell. Biol.* **25**, 8401-8414.

Chen, C. P., Chen, C. Y., Yang, Y. C., Su, T. H. and Chen, H. (2004). Decreased placental GCM1 (glial cells missing) gene expression in pre-eclampsia. *Placenta* **25**, 413-421.

Chuang, H. C., Chang, C. W., Chang, G. D., Yao, T. P. and Chen, H. (2006). Histone deacetylase 3 binds to and regulates the GCMa transcription factor. *Nucleic Acids Res.* **34**, 1459-1469.

Cross, J. C. (2005). How to make a placenta: mechanisms of trophoblast cell differentiation in mice-a review. *Placenta* **26 Suppl. A**, S3-S9.

Cui, J., O'Shea, K. S., Purkayastha, A., Saunders, T. L. and Ginsburg, D. (1996). Fatal haemorrhage and incomplete block to embryogenesis in mice lacking coagulation factor V. *Nature* **384**, 66-68.

Follenzi, A., Ailles, L. E., Bakovic, S., Geuna, M. and Naldini, L. (2000). Gene transfer by lentiviral vectors is limited by nuclear translocation and rescued by HIV-1 pol sequences. *Nat. Genet.* **25**, 217-222.

Fujito, N., Samura, O., Miharu, N., Tanigawa, M., Hyodo, M. and Kudo, Y. (2006). Increased plasma mRNAs of placenta-specific 1 (PLAC1) and glial cells-missing 1 (GCM1) in mothers with pre-eclampsia. *Hiroshima J. Med. Sci.* **55**, 9-15.

Giunta, B., Obregon, D., Hou, H., Zeng, J., Sun, N., Nikolic, V., Ehrhart, J., Shytle, D., Fernandez, F. and Tan, J. (2006). EGCG mitigates neurotoxicity mediated by HIV-1 proteins gp120 and Tat in the presence of IFN-gamma: role of JAK/STAT1 signaling and implications for HIV-associated dementia. *Brain Res.* **1123**, 216-225.

Gottlicher, M., Minucci, S., Zhu, P., Kramer, O. H., Schimpf, A., Giavara, S., Sleeman, J. P., Lo Coco, F., Nervi, C., Pelicci, P. G. et al. (2001). Valproic acid defines a novel class of HDAC inhibitors inducing differentiation of transformed cells. *EMBO J.* **20**, 6969-6978.

Griffin, C. T., Srinivasan, Y., Zheng, Y. W., Huang, W. and Coughlin, S. R. (2001). A role for thrombin receptor signaling in endothelial cells during embryonic development. *Science* **293**, 1666-1670.

Hemberger, M., Himmelbauer, H., Neumann, H. P., Plate, K. H., Schwarzkopf, G. and Fundele, R. (1999). Expression of the von Hippel-Lindau-binding protein-1 (Vbp1) in fetal and adult mouse tissues. *Hum. Mol. Genet.* **8**, 229-236.

Isermann, B., Hendrickson, S. B., Hutley, K., Wing, M. and Weiler, H. (2001). Tissue-restricted expression of thrombomodulin in the placenta rescues thrombomodulin-deficient mice from early lethality and reveals a secondary developmental block. *Development* **128**, 827-838.

Isermann, B., Sood, R., Pawlinski, R., Zogg, M., Kalloway, S., Degen, J. L., Mackman, N. and Weiler, H. (2003). The thrombomodulin-protein C system is essential for the maintenance of pregnancy. *Nat. Med.* **9**, 331-337.

Isermann, B., Vinnikov, I. A., Madhusudhan, T., Herzog, S., Kashif, M., Blautzik, J., Corat, M. A., Zeier, M., Blessing, E., Oh, J. et al. (2007). Activated protein C protects against diabetic nephropathy by inhibiting endothelial and podocyte apoptosis. *Nat. Med.* **13**, 1349-1358.

Kiekhaefer, C. M., Boyer, M. E., Johnson, K. D. and Bresnick, E. H. (2004). A WW domain-binding motif within the activation domain of the hematopoietic transcription factor NF-E2 is essential for establishment of a tissue-specific histone modification pattern. *J. Biol. Chem.* **279**, 7456-7461.

Maltepe, E., Krampitz, G. W., Okazaki, K. M., Red-Horse, K., Mak, W., Simon, M. C. and Fisher, S. J. (2005). Hypoxia-inducible factor-dependent histone deacetylase activity determines stem cell fate in the placenta. *Development* **132**, 3393-3403.

McCaig, D. and Lyall, F. (2009). Hypoxia upregulates GCM1 in human placenta explants. *Hypertens. Pregnancy* **28**, 457-472.

McIntire, D. D., Bloom, S. L., Casey, B. M. and Leveno, K. J. (1999). Birth weight in relation to morbidity and mortality among newborn infants. *N. Engl. J. Med.* **340**, 1234-1238.

Nagy, A., Rossant, J., Nagy, R., Abramow-Newerly, W. and Roder, J. C. (1993). Derivation of completely cell culture-derived mice from early-passage embryonic stem cells. *Proc. Natl. Acad. Sci. USA* **90**, 8424-8428.

Nervi, C., Borello, U., Fazi, F., Buffa, V., Pelicci, P. G. and Cossu, G. (2001). Inhibition of histone deacetylase activity by trichostatin A modulates gene expression during mouse embryogenesis without apparent toxicity. *Cancer Res.* **61**, 1247-1249.

Ohlmann, P., Eckly, A., Freund, M., Cazenave, J. P., Offermanns, S. and Gachet, C. (2000). ADP induces partial platelet aggregation without shape change and potentiates collagen-induced aggregation in the absence of Galphaq. *Blood* **96**, 2134-2139.

Ohlsson, R., Falck, P., Hellstrom, M., Lindahl, P., Bostrom, H., Franklin, G., Ahrlund-Richter, L., Pollard, J., Soriano, P. and Betsholtz, C. (1999). PDGFB regulates the development of the labyrinthine layer of the mouse fetal placenta. *Dev. Biol.* **212**, 124-136.

Okada, Y., Ueshin, Y., Isotani, A., Saito-Fujita, T., Nakashima, H., Kimura, K., Mizoguchi, A., Oh-Hora, M., Mori, Y., Ogata, M. et al. (2007). Complementation of placental defects and embryonic lethality by trophoblast-specific lentiviral gene transfer. *Nat. Biotechnol.* **25**, 233-237.

Palumbo, J. S., Zogg, M., Talmage, K. E., Degen, J. L., Weiler, H. and Isermann, B. H. (2004). Role of fibrinogen- and platelet-mediated hemostasis in mouse embryogenesis and reproduction. *J. Thromb. Haemost.* **2**, 1368-1379.

Pan, Y., Chen, C., Shen, Y., Zhu, C. H., Wang, G., Wang, X. C., Chen, H. Q. and Zhu, M. S. (2008). Curcumin alleviates dystrophic muscle pathology in mdx mice. *Mol. Cells* **25**, 531-537.

Prince, H. M., Bishton, M. J. and Harrison, S. J. (2009). Clinical studies of histone deacetylase inhibitors. *Clin. Cancer Res.* **15**, 3958-3969.

Qiu, Y., Guo, M., Huang, S. and Stein, R. (2004). Acetylation of the BETA2 transcription factor by p300-associated factor is important in insulin gene expression. *J. Biol. Chem.* **279**, 9796-9802.

Rudofsky, G., Jr, Reismann, P., Grafe, I. A., Konrade, I., Djuric, Z., Tafel, J., Buchbinder, S., Zorn, M., Humpert, P. M., Hamann, A. et al. (2007). Improved vascular function upon pioglitazone treatment in type 2 diabetes is not associated with changes in mononuclear NF-kappaB binding activity. *Horm. Metab. Res.* **39**, 665-671.

Sambrano, G. R., Weiss, E. J., Zheng, Y. W., Huang, W. and Coughlin, S. R. (2001). Role of thrombin signalling in platelets in haemostasis and thrombosis. *Nature* **413**, 74-78.

Sato, Y., Fujiwara, H., Zeng, B. X., Higuchi, T., Yoshioka, S. and Fujii, S. (2005). Platelet-derived soluble factors induce human extravillous trophoblast migration and differentiation: platelets are a possible regulator of trophoblast infiltration into maternal spiral arteries. *Blood* **106**, 428-435.

Schorpp-Kistner, M., Wang, Z. Q., Angel, P. and Wagner, E. F. (1999). JunB is essential for mammalian placentation. *EMBO J.* **18**, 934-948.

Schreiber, J., Riethmacher-Sonnenberg, E., Riethmacher, D., Tuerk, E. E., Enderich, J., Bosl, M. R. and Wegner, M. (2000a). Placental failure in mice lacking the mammalian homolog of glial cells missing, GCMa. *Mol. Cell. Biol.* **20**, 2466-2474.

Schreiber, M., Wang, Z. Q., Jochum, W., Fetka, I., Elliott, C. and Wagner, E. F. (2000b). Placental vascularisation requires the AP-1 component fra1. *Development* **127**, 4937-4948.

Schubert, S. W., Abendroth, A., Kilian, K., Vogler, T., Mayr, B., Knerr, I. and Hashemolhosseini, S. (2008). bZIP-Type transcription factors CREB and OASIS bind and stimulate the promoter of the mammalian transcription factor GCMa/Gcm1 in trophoblast cells. *Nucleic Acids Res.* **36**, 3834-3846.

Shivdasani, R. A., Rosenblatt, M. F., Zucker-Franklin, D., Jackson, C. W., Hunt, P., Saris, C. J. and Orkin, S. H. (1995). Transcription factor NF-E2 is required for platelet formation independent of the actions of thrombopoietin/MGDF in megakaryocyte development. *Cell* **81**, 695-704.

Simmons, D. G., Natale, D. R., Begay, V., Hughes, M., Leutz, A. and Cross, J. C. (2008a). Early patterning of the chorion leads to the trilaminar trophoblast cell structure in the placental labyrinth. *Development* **135**, 2083-2091.

Simmons, D. G., Rawn, S., Davies, A., Hughes, M. and Cross, J. C. (2008b). Spatial and temporal expression of the 23 murine Prolactin/Placental Lactogen-related genes is not associated with their position in the locus. *BMC Genomics* **9**, 352.

Sood, R. and Weiler, H. (2003). Embryogenesis and gene targeting of coagulation factors in mice. *Best Pract. Res. Clin. Haematol.* **16**, 169-181.

Sood, R., Zogg, M., Westrick, R. J., Guo, Y. H., Kerschen, E. J., Girardi, G., Salmon, J. E., Coughlin, S. R. and Weiler, H. (2007). Fetal gene defects precipitate platelet-mediated pregnancy failure in factor V Leiden mothers. *J. Exp. Med.* **204**, 1049-1056.

Steingrimsson, E., Tessarollo, L., Reid, S. W., Jenkins, N. A. and Copeland, N. G. (1998). The bHLH-Zip transcription factor Tfeb is essential for placental vascularization. *Development* **125**, 4607-4616.

Sun, W. Y., Witte, D. P., Degen, J. L., Colbert, M. C., Burkart, M. C., Holmback, K., Xiao, Q., Bugge, T. H. and Degen, S. J. (1998). Prothrombin deficiency results in embryonic and neonatal lethality in mice. *Proc. Natl. Acad. Sci. USA* **95**, 7597-7602.

Tachibana, H., Koga, K., Fujimura, Y. and Yamada, K. (2004). A receptor for green tea polyphenol EGCG. *Nat. Struct. Mol. Biol.* **11**, 380-381.
Tanaka, S., Kunath, T., Hadjantonakis, A. K., Nagy, A. and Rossant, J. (1998). Promotion of trophoblast stem cell proliferation by FGF4. *Science* **282**, 2072-2075.
Toomey, J. R., Kratzer, K. E., Lasky, N. M., Stanton, J. J. and Broze, G. J., Jr (1996). Targeted disruption of the murine tissue factor gene results in embryonic lethality. *Blood* **88**, 1583-1587.
Wilting, R. H., Yanover, E., Heideman, M. R., Jacobs, H., Horner, J., van der Torre, J., DePinho, R. A. and Dannenberg, J. H. (2010). Overlapping functions of Hdac1 and Hdac2 in cell cycle regulation and haematopoiesis. *EMBO J.* **29**, 2586-2597.
Xu, M. J., Matsuoka, S., Yang, F. C., Ebihara, Y., Manabe, A., Tanaka, R., Eguchi, M., Asano, S., Nakahata, T. and Tsuji, K. (2001). Evidence for the presence of murine primitive megakaryocytopoiesis in the early yolk sac. *Blood* **97**, 2016-2022.
Xue, J., Wu, Q., Westfield, L. A., Tuley, E. A., Lu, D., Zhang, Q., Shim, K., Zheng, X. and Sadler, J. E. (1998). Incomplete embryonic lethality and fatal neonatal hemorrhage caused by prothrombin deficiency in mice. *Proc. Natl. Acad. Sci. USA* **95**, 7603-7607.

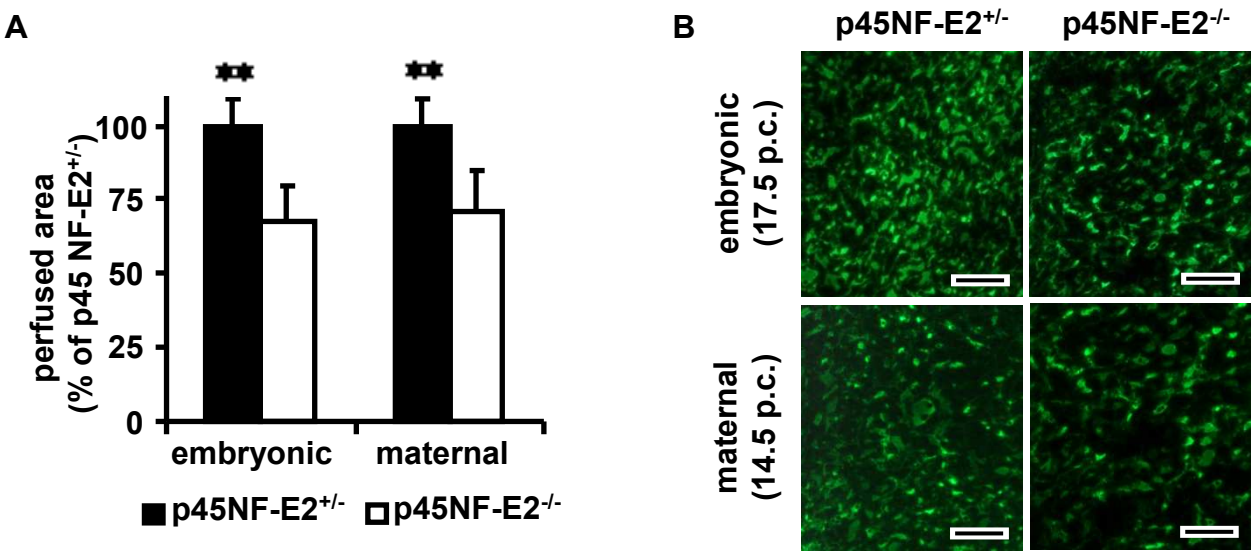
A
**
**
perfused area
(% of p45 NF-E2+/-)
100
75
50
25
0
embryonic
maternal
p45NF-E2+/-
p45NF-E2-/-
B
p45NF-E2+/-
p45NF-E2-/-
embryonic
(17.5 p.c.)
maternal
(14.5 p.c.)

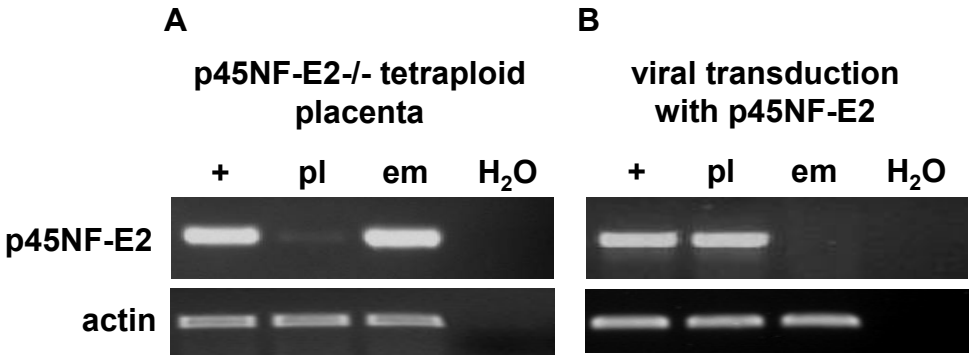
A
p45NF-E2-/- tetraploid placenta
+
pl
em
H2O
p45NF-E2
actin
B
viral transduction with p45NF-E2
+
pl
em
H2O

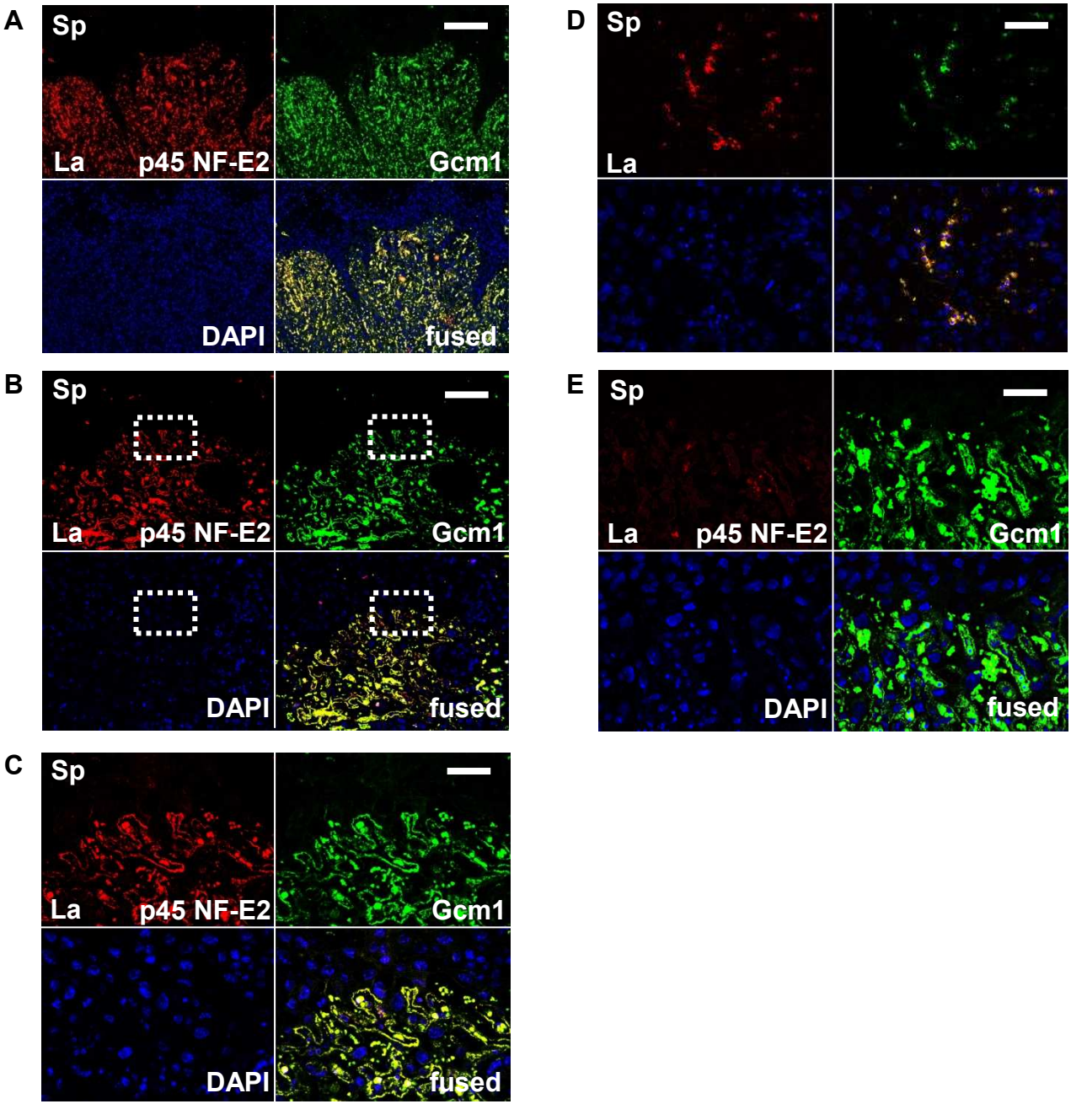
A
Sp
La
p45 NF-E2
Gcm1
DAPI
fused
B
Sp
La
p45 NF-E2
Gcm1
DAPI
fused
C
Sp
La
p45 NF-E2
Gcm1
DAPI
fused
D
Sp
La
E
Sp
La
p45 NF-E2
Gcm1
DAPI
fused

A

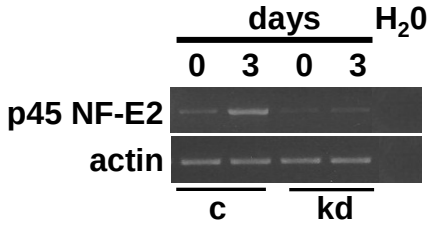
days
H20
0 3 0 3
p45 NF-E2
actin
c
kd

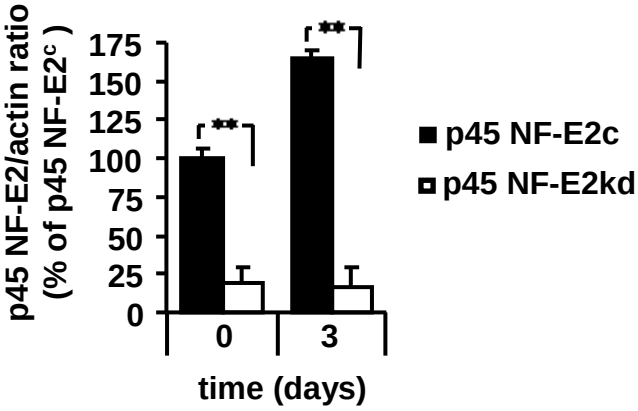
p45 NF-E2/actin ratio
(% of p45 NF-E2c)
175
150
125
100
75
50
25
0
**
**
0
3
time (days)
p45 NF-E2c
p45 NF-E2kd

B

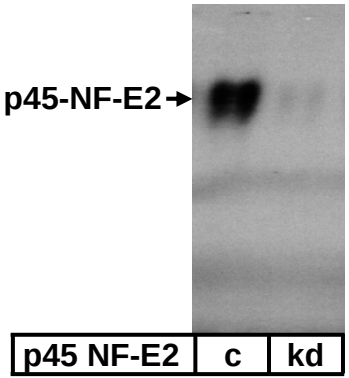
p45-NF-E2
p45 NF-E2
c
kd

Table S1. Embryonic and placental development

Gestational age (dpc)	*p45NF-E2* genotype	*n*	Embryonic length (mm)	Embryonic weight (mg)	Placental weight (mg)	Placental area (mm^2)
10.5	+/–	30	5.0±0.01	26±3	59±1	74±1
	–/–	37	5.1±0.01	26±2	51±1	74±1
12.5	+/–	40	8.9±0.02	114±4	106±4	202±2
	–/–	36	8.8±0.02	110±6	105±6	203±4
14.5	+/–	64	11.1±0.02	305±5	109±5	204±5
	–/–	70	11.3±0.03	306±4	108±4	205±3
16.5	+/–	27	16.6±0.01	665±9	100±5	173±5
	–/–	32	15.9±0.02*	640±7*	101±7	174±2
17.5	+/–	50	19.8±0.02	1003±9	101±3	176±3
	–/–	43	16.5±0.02**	911±8**	104±4	174±4

Embryonic length and weight as well as placental weight and area (embryonic aspect of the placenta) as a function of pregnancy duration. Mean ± s.e.m. *, $P<0.05$; **, $P<0.01$; ANOVA.